SIEMENS
Westinghouse

August 8, 2003

Mr. Brian Benney
Project Manager, Section 2
Project Directorate IV
Division of Licensing Project Management
Document Processing Center, Mail Stop 07E1
United States Nuclear Regulatory Commission
Washington, DC 20555-0001

Subject: Siemens Westinghouse Power Corporation, "Missile Probability Analysis of BB81/281 13.9m^2", TAC No. MB7964.

Dear Brian:

Attached please find RAI questions submitted by the NRC for the BB81/281 13.9m2 missile analysis and responses provided by Siemens Westinghouse (Attachment 1). One of the questions was answered by providing a technical paper recently prepared on the benefit of compressive residual stresses for nuclear rotor discs. This paper is included as Attachment 2.

The original Topical Report we submitted, CT-27332 Revision 0, has been revised to be in full compliance with the NRC recommendations in the Safety Evaluation (SE) report. This revised report CT-27332 Revision 2 is enclosed as Attachment 3.

Regards,

Peter Bird

Peter Bird
Field Service Engineering S326
Siemens Westinghouse Power Corporation
Phone: (407) 736-4686

Enclosures:

1) RAI for Topical Report, "Missile Probability Analysis of BB81/281 13.9m2", Siemens Westinghouse Power Corporation, Response Submitted August 8, 2003.
2) Walter David, Dr. Andreas Feldmueller, Dr. Heinrich Oeynhausen, "Shrunk on Disk Technology in Large Nuclear Power Plants – the Benchmark against Stress Corrosion Cracking", to be

T010

presented at the Parsons Conference, September 16-18, 2003, Dublin, Ireland, Siemens Power Generation.

3) "Missile Probability Analysis for BB81/281 13.9m2", by P. Bird and Dr. A. Bagaviev, August 8, 2003, CT-27332 Revision 2, Siemens AG – Power Generation.

cc: James McCracken S326
Jim Auman S326
Andreas Feldmueller S327
Dr. Albert Bagaviev S321

RAI FOR
TOPICAL REPORT
"MISSILE PROBABILITY ANALYSIS OF BB81/281 13.9M^2"
SIEMENS WESTINGHOUSE POWER CORPORATION
Response Submitted August 8, 2003

(1) The staff's position regarding acceptable values for some key deterministic and probabilistic parameters used in a typical turbine missile analysis considering disk burst and casing penetration was stated in a safety evaluation (SE) of Siemens turbine missile methodology dated April 2, 2003. A list of these parameters is provided below:

Standard deviation for K_{IC}
Initial crack depth
Maximum mean K_{IC}
Maximum crack depth for considering crack branching
Mean value for the crack branching factor
Standard deviation for the crack branching factor
Bore stresses due to shrink fit with no record
Friction coefficient
Plant-specific parameters

Please identify the parameters in your current analysis that assumed different values or probabilistic distributions than their corresponding ones accepted by the staff in the April 2, 2003 SE and assess the impact of the differences on your results and conclusion.

Response:
Unfortunately, the 13.9m^2 missile analysis documented in CT-27332 Revision 0 was performed in the Fall of 2002, the original Missile Report issued in February 2003 and the NRC Safety Evaluation (SE) in April 2003. Because of these time differences, there are differences in the input parameters used and those recommended by the NRC staff in the SE. As summarized in the attached tabulation, the two input parameters that were not consistent with the NRC staff recommendations are maximum crack depth for considering crack branching and friction coefficient in the casing penetration calculations.

With regard to maximum crack depth for considering crack branching, the missile analysis has been revised to use the 3-inch criterion. Reference Revision 2 of CT-27332 as attached in a separate document. This revised report complies with all of the NRC recommendations for input parameters.

The casing penetration analysis used in CT-27332 Revision 0 is the same existing analysis used for the Limerick design, which applies and is discussed in ER9605 (one of the submittals to the NRC). This analysis used a friction coefficient of 0.40. Use of a 0.25 friction factor per latest NRC recommendation results in increased casing penetration probabilities for each disc. Revision 2 of CT-27332 includes the effect of the 0.25 friction coefficient in the missile energy calculations.

A sensitivity study was performed for the purpose of evaluating the effect of friction coefficient on casing penetration probability. Results are summarized on the following figure. Calculations were made for each of the three discs at friction coefficients of 0.40 (same as Limerick), 0.10 and zero. The zero case was made assuming no friction between disc fragments, blades and casings during energy dissipation within the LP turbine after burst.

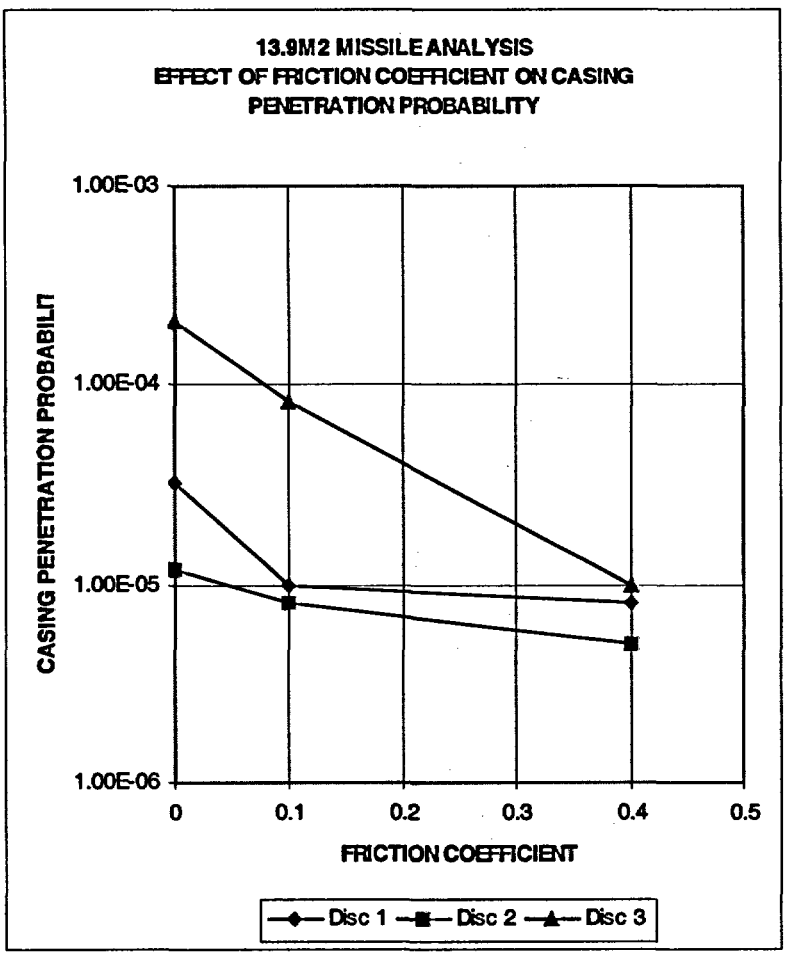

Input value	Value used in original analysis, Revision 0 of CT-27332	Value used in revised analysis, Revision 2 of CT-27332	NRC acceptable values
Standard deviation for K_{IC}	As stated in Section 3.4.3, minimum value of 150 ksi$\sqrt{in}$ (165 MPa$\sqrt{m}$) and maximum value of 236 ksi$\sqrt{in}$ (260 MPa$\sqrt{m}$) were used.	A standard deviation of 10% was used. Complies with NRC criteria.	Based on three standard deviations of 10% from maximum mean value of 200 ksi$\sqrt{in}$, the acceptable range would be minimum of 140 ksi$\sqrt{in}$ and maximum of 260 ksi$\sqrt{in}$.
Initial crack depth	As stated in Section 3.4.6, a value of 0.12 inch (3 mm) was used.	A value of 0.12 inch (3 mm) was used. Complies with NRC criteria.	0.12 inch is the accepted value.
Maximum mean K_{IC}	The mean value was 193 ksi$\sqrt{in}$ (212.5 MPa$\sqrt{m}$).	A mean value of 200 ksi$\sqrt{in}$ (219.8 MPa$\sqrt{m}$) was used. Complies with NRC criteria.	Maximum acceptable upper shelf mean is 200 ksi$\sqrt{in}$.
Maximum crack depth for considering crack branching	As stated in Section 3.4, a 4-inch (100-mm) criterion was used.	The 3-inch criterion was used. Complies with NRC criteria.	A 3-inch criterion is accepted.
Mean value for the crack branching factor	As stated in Section 3.4.2, a mean of 0.65 was used.	A mean of 0.65 was used up to 3-inch. Complies with NRC criteria.	A mean value of 0.65 is accepted up to the 3-inch criterion.
Standard deviation for the crack branching factor	As stated in Section 3.4.2, a standard deviation of 0.175 was used.	A standard deviation of 0.175 was used up to 3-inch. Complies with NRC criteria.	A standard deviation of 0.175 is accepted up to the 3-inch criterion.
Bore stresses due to shrink fit with no record	As shown in Table 2, tangential bore stresses with shrink fit included are 72 ksi (498 MPa), 76 ksi (521 MPa) and 78 ksi (535 MPa) for discs 1, 2 and 3 respectively. These discs have material certification records.	Same as Revision 0. Complies with NRC criteria.	The minimum accepted bore stress with shrink fit included and no material certification record is 55 ksi.
Friction coefficient	Existing casing penetration calculations from the Limerick Missile Report, ER9605, were used with a friction coefficient of 0.40.	A friction coefficient of 0.25 was used. Complies with NRC criteria.	The accepted friction coefficient is 0.25.
Plant-specific parameters	In the case of the 13.9m^2 design, SWPC as OEM knows these input parameters. Processing these inputs within the PDMISSILE calculations remains the same.	Same as Revision 0. NRC criteria do not apply in this case.	In the case of GE rotor discs, these input parameters are not known to SWPC ahead of time and must be derived by measurement during an outage.

(2) Section 3.3 and Figure 8 present the residual stress distribution due to manufacturing without adequate explanation. Please provide basis for this residual stress distribution, e.g., analytical (FEM) results with experimental verification. Also, the effective stresses should include tensile stresses due to shrink-fit. Update Figure 8 to reflect this modification, and assess its impact on your results and conclusion.

Response:

Attachment 1: Siemens technical paper "Shrunk on Disk Technology in Large Nuclear Power Plants – the Benchmark against Stress Corrosion Cracking", to be presented at the upcoming Parson's Conference of September 16-18, 2003 in Dublin.

This paper provides the most current basis for residual stress distribution along with analytical results and experimental verification. Figure 14 in the technical paper superimposes the centrifugal forces, tensile stresses due to shrink fit and residual stresses, as requested. The result is essentially the same conclusion as presented in Figure 8 of CT-27332 for BB81/281 13.9m^2 LP turbines. The only difference is that Figure 8 is based on results at 120% of rated speed, whereas Figure 14 in the technical paper is based on results at rated speed. Therefore, we believe that Figure 8 applies and does not need to be updated.

(3) Section 3.4.7.1 mentions that "...using standard statistical evaluation procedures, the crack initiation probabilities at 90% confidence level for the #1 disks are as shown in Table 2." Provide information regarding this standard statistical evaluation procedure. The information should include the number of indications, the number of reactor years or the number of disks, and the assumed probability distribution (e.g., log-normal or binomial).

Response:

For large values of N (disk number) or small values of n (disks with flaws), the estimated probability of crack initiation "p" is small ($p < 0.1$), and the binomial distribution can be approximated by a Poisson distribution.

The bounds for the Poisson parameter λ at a confidence level of 90% are [0.1; 3.89] for 1 indication (among 82 #1 disks) and [0.53; 5.3] for 2 indications (among 324 back end disks), independent on the sample size N.

The upper value of the Poisson parameter at 90% Confidence Level for $n = 1$, $\lambda = 3.89$ and with $N = 82$:

$$p = (\lambda / N) = (3.89 / 82) = 0.047$$

The upper value of the Poisson parameter at 90% Confidence Level for $n = 2$, $\lambda = 5.3$ and with $N = 324$:

$$p = (\lambda / N) = (5.3 / 324) = 0.0164$$

(4) The energy equation in section 4.1.1 is not correct. Please revise it.

Response:

Revision 2 of CT-27332 corrects this error.

(5) Section 4.1.3 calculation results for "ductile fracture" of disks. Confirm that the ductile fracture methodology is the same as ductile burst methodology that the NRC reviewed as related to the April 2, 2003 SE. If ductile fracture means J integral – fracture resistance (J-R) approach, then you need to provide details. Likewise, confirm that the probability of overspeed was calculated in accordance with ER-504, and provide additional information if it is not.

Response:

This is a wording issue only. The approach is the same as the ductile burst methodology presented and approved in the April 2, 2003 SE. We confirm that the probability of overspeed was calculated in accordance with ER-504.

In summary, we believe that the 13.9m^2 missile analysis as documented in CT-27332 Revision 2 complies with all of the NRC criteria identified in the Safety Evaluation (SE) dated April 2, 2003.

Shrunk on Disk Technology in Large Nuclear Power Plants - the Benchmark against Stress Corrosion Cracking

Walter David, Dr. Andreas Feldmüller and Dr. Heinrich Oeynhausen
Siemens Power Generation

Introduction

The modernisation of steam turbines to improve plant efficiency plays an important role in reaching the targets set at Kyoto.

Especially blades, developed in the last years, combined with new sealing technologies and turbine casings with optimised flow paths[1] are key factors for ecological, as well as economical, improvements of a power plant.

Regarding the modernisation of power plants, along with efficiency is the issue of reliability of the equipment a driving force.
In the last decades, many turbines, especially in nuclear plants, were affected by stress corrosion cracking (SCC), mainly in the large LP rotors[2].

Repair work is often time consuming and neither supports the economics nor solves general design deficiencies. Therefore newly designed equipment, applying latest technology to improve reliability, as well as efficiency, is often a more advantageous option.

As large half speed (1500/1800RPM) LP turbines were first developed in the late 60s, qualified monoblock rotors were not available in the required sizes. Therefore most of the turbine suppliers started to develop LP turbines with shrunk on disk designs.

Although the basic principle was the same, the design details of the suppliers were extremely different and varied widely in their ability to avoid SCC from excellent to poor, i.e., strongly affected by SCC. Figure 1 shows typical problems with stress corrosion cracking found on shrunk on disk rotors in the past [2]. All major manufacturers worldwide, except one, had to improve their design due to a large numbers of reported failures which led to the shrunk on disk generally receiving a poor design reputation. Because of this, most suppliers converted to using monoblock rotors as their design principle, based on improvements in large forgings, or welded rotors.

This paper will show that in contrast to this, a shrunk on disk rotor is not just an alternative design, but rather should be regarded as the benchmark for all other nuclear LP rotor designs.

With a closer examination of the background of the SCC phenomenon, it will be clear to all that the design details are the distinguishing factors and not the design principle itself. This notion is supported by the fact that the turbines built with the technology described in this paper did not experience an SCC problem. This technology was chosen to replace LP turbine rotors built by various original equipment manufacturers, including all varieties of design principles, such as:

–Shrunk on disk [3]
–Monoblock [4]
–Welded disk

The reason for the replacement of these rotors was the gain in efficiency and power, but often a reliability problem (e.g., SCC in the blade attachments) was an additional reason for the modernisation.

Examples of these different designs which have been replaced by the advanced shrunk on disk rotor design developed by Siemens PG can be seen in Figure 2.

Design history of the Advanced Shrunk on Disk Rotors

The original Siemens KWU shrunk on disk designs for large nuclear LP turbines were based on ten disks per rotor (see Figure 3). With the advanced shrunk on disk rotor designs the number of disks per flow was reduced as this was found to be beneficial for efficiency, as well as SCC prevention. As an example, the larger first disk, allows for an increased number of blade stages to reduce stage loading and increase blade efficiency. Moreover the compressive stresses applied during heat treatment (see below) benefit from this design modification.

On top of the reduced number of disks, it was found that in the last two disks per flow, anti-rotation keys were not required if a sufficient shrink fit was applied.

The following portion of this paper describes the SCC phenomenon and the preventative measures to avoid SCC attacks on the rotor components.

Stress Corrosion Cracking of Turbine Disks

In Figure 4, the factors influencing the stress corrosion cracking behaviour (SCC) and the Siemens measures to avoid SCC are summarized. Although Siemens KWU low-pressure turbines were not affected by stress corrosion cracking, they began extensive studies into the causes and prevention of stress corrosion cracking as a precautionary measure in the early 80's.

Material Parameters

The quenched-and-tempered alloy steels that were investigated had different amounts of nickel, chromium, molybdenum and vanadium. Also considered were various degrees of purity including steels with segregations and elevated inclusion content and a "super-clean" variant. Some steels were tempered at different temperatures to achieve 0.2% yield strength levels between 700 and 1250 MPa.

Laboratory Studies of Stress Corrosion Cracking

Siemens PG studied the stress corrosion cracking in steam turbine disk steels as a function of water chemistry and various material parameters, such as strength, chemical composition, steel purity, melting process, etc. High-purity water with a conductivity of < 0.2 µS/cm, both deoxygenated (oxygen < 10 ppb) and oxygen saturated, at temperatures of up to 150°C, was used as the corrosive medium. To simulate irregularities in the water steam cycle, gaseous and other types of impurities were added to increase conductivity.

Stress Corrosion Crack Initiation

In high-purity water with a conductivity of < 0.2 µS/cm, only the quenched-and-tempered condition, i.e., the hardness of the steel, influences initiation of stress corrosion cracking. Up to a 0.2% yield strength of 970 MPa, stress corrosion cracking did not initiate cracking in any of the quenched-and-tempered conditions studied. Nor did it cause cracking in smooth or notched test pieces at stresses above the 0.2% yield strength (Figure 5).[5-7] This is independent of the purity of the steel. In high-purity water, those steels conventionally melted 25 years ago perform just as well as high-purity steels made using the ESR process.[8] Under high purity water conditions, even non-metallic inclusions (such as Al_2O_3, MnS, etc.) in the surface of the material do not act as crack initiators and have no effect on stress corrosion cracking resistance. This holds true in both pure oxygen and oxygen-saturated water. No localized, anodic dissolution on the material surface (pit formation) was observed under these high-purity corrosion conditions.

Under quenched-and-tempered conditions the steels with a 0.2% yield strength > 1085 MPa were damaged by hydrogen-induced stress corrosion cracking (Figure 5).

Stress Corrosion Crack Propagation

The two phases, crack initiation and crack propagation, must be looked at separately with stress corrosion cracking. As stated above, stress corrosion cracking does not initiate in either smooth or notched specimens in high-purity water. However, stress corrosion does result in crack propagation in statically loaded fracture mechanics test specimens with very sharp, deep cracks in high-purity water.

Crack propagation results are shown in Figure 6. As with crack initiation, there is a 0.2% yield strength threshold between 1000 and 1100 MPa above which the mechanism, and subsequently the crack propagation rate, drastically changes. With 0.2% yield strength between 650 and 1085 MPa, propagation rates for stress corrosion cracking are almost entirely independent of strength. At a service temperature of 80°C, a crack would, depending on the material's strength, propagate by 0.2 to 0.8 mm per year due to stress corrosion cracking.

Higher aggressiveness in the media only has a slight influence on crack propagation since the electrolyte in the crack is almost decoupled from the surrounding medium and nearly constant electrolyte conditions are established at the crack tip.[6, 7]

When the 0.2% yield strength exceeds roughly 1100 MPa, the crack propagation rate increases drastically by several powers of ten. In this strength range, hydrogen-induced cracking plays a decisive role during crack propagation.

In summary, whereas crack initiation does not occur in high-purity water at 0.2% yield strength below roughly 1000 MPa, existing cracks will propagate also under high purity water conditions due to stress corrosion cracking. Cracks which have initiated in media with elevated conductivity can therefore continue to propagate even if high-purity water is present outside the crack.

Therefore the maximum allowable service stresses, to avoid stress corrosion crack initiation, under different steam and water conditions must be defined.

Threshold Values to Prevent SCC Initiation

Our own results and data from the literature regarding studies of stress corrosion cracking initiation in low-alloy quenched-and-tempered steels for steam turbine disks with 0.2% yield strength <1000 MPa are summarized and discussed below. The goal was to define stress limits for the prevention of stress corrosion crack initiation as a function of the corrosive medium.

The results in high purity water are summarized in Figure 7.[5-8, 10, 11] Since no stress corrosion cracking occurred, the limit stress for the prevention of crack initiation has been conventionally defined as

R_{SCCI} (high-purity water) = 1.1

(R_{SCCI} [service stress/0.2% yield strength] = threshold value for preventing stress corrosion crack initiation in rotor steels 0.2% yield strength <1000 MPa).

Figure 7 also includes results of stress corrosion crack initiation studies in condensing steam.[11-13] These studies simulate conditions as can occur during operation in the region of the Wilson line. In this region, the condensate first forms on the surface of the material. Because of the coefficients of distribution, enriched concentrations of water-soluble impurities in the water/steam cycle can occur here and cause pitting and crack initiation.

R_{SCCI} (condensing steam) = 0.9

Similar Threshold curves as shown in Figure 7 were developed with data under more aggressive corrosion conditions, such as

- condensing steam with crevice conditions [11]
- water with gaseous impurities [5, 6, 8, 10, 14]

- stagnant water without refreshing [6-8, 10, 14]

This simulates strong increase in conductivity, which however is not typical for normal operating conditions. In these relatively aggressive media for low-alloy steel, high stresses are likewise required to produce stress corrosion cracking. The majority of test specimens exhibited no stress corrosion cracking with stress/0.2% yield strength ≥ 0.9.

Even in 30% NaOH solutions at 100 –120°C, the SCC-initiation time is still clearly dependent on stress.[15-17] Crack initiation can therefore be precluded even during short disturbances if the associated service stresses remain below 50 to 60% of the 0.2% yield strength:

R_{SCCI} (aggressive medium conditions) = 0.5 - 0.6

Figure 8 provides a summary of which stress limits must be exceeded to initiate stress corrosion cracks in low-alloy quenched-and-tempered steels for steam turbine rotors with a 0.2% proof stress < 1000 MPa. These stress limits are independent of the material parameters chemical composition, steel purity, surface inclusions or similar metallurgical factors as can occur with heats produced using conventional industrial techniques. This includes surface imperfections, such as mechanical notches, surface scratches and comparable surface damage as can occur in singular cases despite careful processing and stringent quality assurance measures.

Use of Compressive Residual Stresses

One possibility for minimizing the stresses in critical regions of components is to induce compressive residual stresses in the material surface. As part of a larger research project, various surface treatment processes were tested and refined with the objective of ensuring compressive residual stresses of sufficient magnitude and depth of penetration without adversely affecting the surface. In the Siemens design the following methods are used to produce surface compressive residual stresses:

Special Heat treatment process

During the heat treatment of the disks, a special water spraying treatment process is used to produce compressive residual stresses in the surface area of the disk. The depth of the compressive residual layer is adjusted in such a way that the machined and finished disk still has near surface compressive residual stresses of up to a depth of more than 50 mm (Figure 9).

Machining and Shot Peening

To reduce the potential for stress corrosion cracking, the machining of the grooves and the entire rim section of the disks have been optimized to minimize residual tensile surface stresses at any particular location. In nearly all cases after machining, a thin layer of compressive residual stresses exists. In the rotor sections which could possibly be exposed to stress corrosion, the disk surfaces, and certain sections of the blade attachment zone, are additionally shot peened to produce deeper compressive surface residual stresses (Figure 10).

Rolling of the keyways

After the shrinking of the disks, the keyway bores are drilled, followed by a rolling and honing procedure. This honing process guarantees the maximum level of compressive residual stresses directly at the surface (Figure 11).

Compressive Residual Stresses and Stress Corrosion Crack Initiation

Comparative studies of stress corrosion cracking were performed on test specimens with rolled and non-rolled bores. Tests were performed in sodium hydroxide to study the mechanism of anodic crack tip dissolution while cathodic polarization was used to simulate the mechanism of hydrogen-induced cracking. In the non-rolled test specimens, the stresses in the bore were on the same order of magnitude as the 0.2% yield strength. For the tests with compressive residual stresses, the test specimens were first pre-stressed to the 0.2%

yield strength (simulating shrink fit), cold-rolled and then stressed again to establish a stress level in the surface of 40% the 0.2% yield strength. The established stresses were subsequently significantly greater than those occurring in shrunk on disks with rolled keyways under service conditions. The results of these studies are shown in Figure 12. Due to the severe corrosion conditions, all of the test specimens which had not been rolled exhibited more-or-less deep stress corrosion cracking after short period. The test pieces with compressive residual stresses produced by rolling were removed after approx. 4.000 – 8.000 hours. All the rolled specimens were free of SCC-cracks.

Crack initiation did not occur in the rolled test specimens. Due to the rolling process, the total surface stress was below the limit for crack initiation R_{scci} = 0.5 - 0.6 (severe corrosion conditions).

As mentioned above, the total service stresses in the keyways are much lower than in the tested, rolled specimens. Due to drilling and rolling after the shrinking process and the high compressive residual stresses resulting from rolling, the total service stresses are still compressive. Moreover, the design avoids shrink fit stresses in the keyway area. The geometry of the shrink fit region is designed in such a way that the keyway is open to the ambient steam. That means steam or condensed steam continuously is exchanged, thus stagnant or crevice conditions with higher conductivity are avoided (Figure 13).

Reduced operating stresses

In addition to the locally optimised design in the keyway area, the global geometry of the disks has been designed to reduce all tensile surface stresses to the target level. Figure 14 shows a typical tangential stress distribution of a first disk at the rated speed. The superimposed stresses given by the advanced heat treatment of the disks, and the sum of both, are also shown in this figure.

Verification in the Field

For many years, Siemens' original design of shrunk on disk rotors, as well as the advanced disk design, have demonstrated and proven the quality of this technology. The total number of fleet operating hours is more than 2,750,000, which have led to more than 40 million disk operating hours, bearing in mind that each unit consists of two to three LP turbine elements with six to ten disks each.

The oldest rotors, which were never replaced, have been in operation for approximately 225,000 operating hours , and the inspections of the disks performed after more than 200,000 hours showed no crack at all.

The same encouraging result was gained in more than 660 disk inspections, with just a single exception in which a SCC crack was detected, now more than 15 years ago.[18]

The subsequent investigations showed that small particles in the finished surface were responsible for the crack initiation. This disk was manufactured more than 25 years ago, at a time when the reasons for SCC were not known in detail. The optimisation of the quality controlled manufacturing process and the developed knowledge of SCC ensured the avoidance of similar events.

Due to this impressive operational record and the availability of new blade and seal designs for improving the turbine efficiency, turbine modernisations were performed in order to optimise the cost effectiveness of the plants with advanced disk technology.

Excellent results were obtained in the German 1400MW nuclear power plant, Emsland, in May 2000. [19] In only 16 days, two LP inner casings and rotors, including re-work of the outer casing, were able to be fully completed. Additional 32MW showed the success of this modernisation by the fact that the guarantees were fully met. It has to be noted that this improvement took place despite the fact that the size of the last stage blades remained constant.

New Products

Many of the turbines originally designed by Siemens have been modernised in order to improve efficiency. Furthermore, products have been made available to improve non OEM turbines like in Figure 2 with the advanced disk design.
Figure 15 shows the advanced shrunk on disk LP rotor, designed for Westinghouse LP turbines BB81 and BB281, including all major design features described in this paper. These include the following factors:

- Compressive residual stresses by heat treatment, shot peening and rolling.
- Optimised disk and keyway design to minimise tensile stresses.
- Reduced number of disks and keys.

Conclusion

The Siemens shrunk on disk rotor technology has proven its reliability during long-term operation periods exceeding 30 years. In addition, the advanced disk rotor design employs further protection measures that thwart the onset of SCC. Based on these design features, new products have been presented to the market which allow the use of this superior technology, to modernise the Siemens Westinghouse fleet, not to mention units built by other turbine manufacturers.

References:

1. M. Deckers, D. Doerwald, 1997, "Steam turbine flow path optimizations for improved efficiency", Power-Gen Asia '97, Singapore, September 9-11, 1997

2. EPRI Report NP-2429, "Steam Turbine Disk Cracking Experience", Volume 1 through 7, Research Project 1398-5, June 1982

3. Smiarowski, M. W., Green, R. C., "Turbine steam path retrofit project completed at PECO nuclear's Limerick generating station units 1 and 2", PowerGen International, New Orleans, 1999.

4. J. A. Bartos, M. S. Gorski, L. E Olah,. M. W. Smiarowski , "Susquehanna steam electric station turbine retrofit/generation uprate: Decision factors for long term reliability and improved performance" PowerGen International, Las Vegas, 2001

5. Engelke,W., Schleithoff,K., Jestrich,H.A., Termuehlen,H., "Design,Operating and Inspection Considerations to Control Stress Corrosion of LP Turbin Disks.", American Power Conference, Chicago, Illinois, April 18-20,1983.

6. David,W., Schleithoff,K., Schmitz,F., "Spannungsrißkorrosion in hochreinem Wasser von 3-3,5% NiCrMoV-Vergütungsstählen für Dampfturbinen-Scheiben und -Wellen.", Teil 1 und 2, Mat.-wiss. u. Werkstofftech. 19, 43-50, 95-104, 1988.

7. Oeynhausen,H., Röttger,G., Ewald,J., Schleithoff,K., Termuehlen,H., "Reliable Disk-Type Rotors for Nuclear Power Plants.", American Power Conf., Chicago, April 27-29, 1987.

8. David,W., Schleithoff,K., Schmitz,F., Ewald,J. , "Stress Corrosion Cracking Behaviour of Turbine Rotor Disk Materials, Crack Initiation and Propagation, Measures to Prevent SCC.", High Temperature Materials for Power Engineering 1990, September 24-27, 1990, Liege-Belgium, 577-588.

9. David,W., Röttger,G., Schleithoff,K., Hamel,H., Termühlen,H. , "Disk-Type LP Turbine Rotor Experience.", Presented at the 1993 International Joint Power Conference, Kansas City, Missouri, Published by the ASME Power Division.

10. Termuehlen,H., Schleithoff,K., Neumann,K. , "Advanced Disk-Type LP Turbine Rotors.", EPRI Workshop, Stress Corrosion Cracking in Steam Turbines, Charlotte, North Carolina, October 10-11, 1990.

11. Roberts,B.W., Greenfield,P. , "Stress Corrosion of Steam Turbine Disk and Rotor Steels.", Corrosion-NACE, Vol 35, No. 9, September, 1979, 402-409.

12. Holdsworth,S.R., Burnell,G., Smith,C., "Factors Influencing Stress Corrosion Crack Initiation in Super Clean 3.5NiCrMoV Rotor Steel.", Superclean Rotor Steels, Work. Proc. Sapporo, Japan, 30-31 August 1989, 299-319.

13. Holdsworth,S.R., Burnell,G., "Stress Corrosion Crack Initiation in LP Turbine Rotor Steels.", High Temperature Materials for Power Engeneering, Liege, Belgium, 2427 Sep. 1990, 555-566.

14. Tavast,J., "Initiation of Stress Corrosion cracking in LP-Rotor Materials.", COST 505, Final Report Project SI, 20.01.89.

15. Speidel,M.O., "Stress Corrosion Cracking in Steam Turbine Rotors, Effects of Materials, Environments and Design.", EPRI Seminar on Low Pressure Turbine Disk Integrity, Dec. 1-2, 1983, San Antonio, Texas.

16. Bertilsson,J.E., Scarlin,B., "Betriebssicherheit von Niederdruck-Dampfturbinenwellen unter SpannungsrißKorrosionsbedingungen.", Brown Boveri Mitlt. 3/4-84, 169-174.

17. Scarlin,R.B., Denk,J., "Stress Corrosion Cracking Behaviour of a Clean 3.5~ NiCrMoV-Steel in Comparison toConventionell Steels.", Superclean Rotor Steels, Work.Proc. Sapporo, Japan, 30-31 August 1989, 263-284.

18. Jacobsen,G., Oeynhausen,H., and Termuehlen,H., "Advanced LP Turbine Installation at 1300 MW Nuclear Power Station Unterweser.", American Power Conf., Chicago, April 29 - May 1, 1991.

19. H. P. Claßen, H. Oeynhausen, J. Riehl, 2001, "Upgrading of the low-pressure steam turbines of nuclear power plants", Siemens Power Journal 1/2001, pp. 26-29.

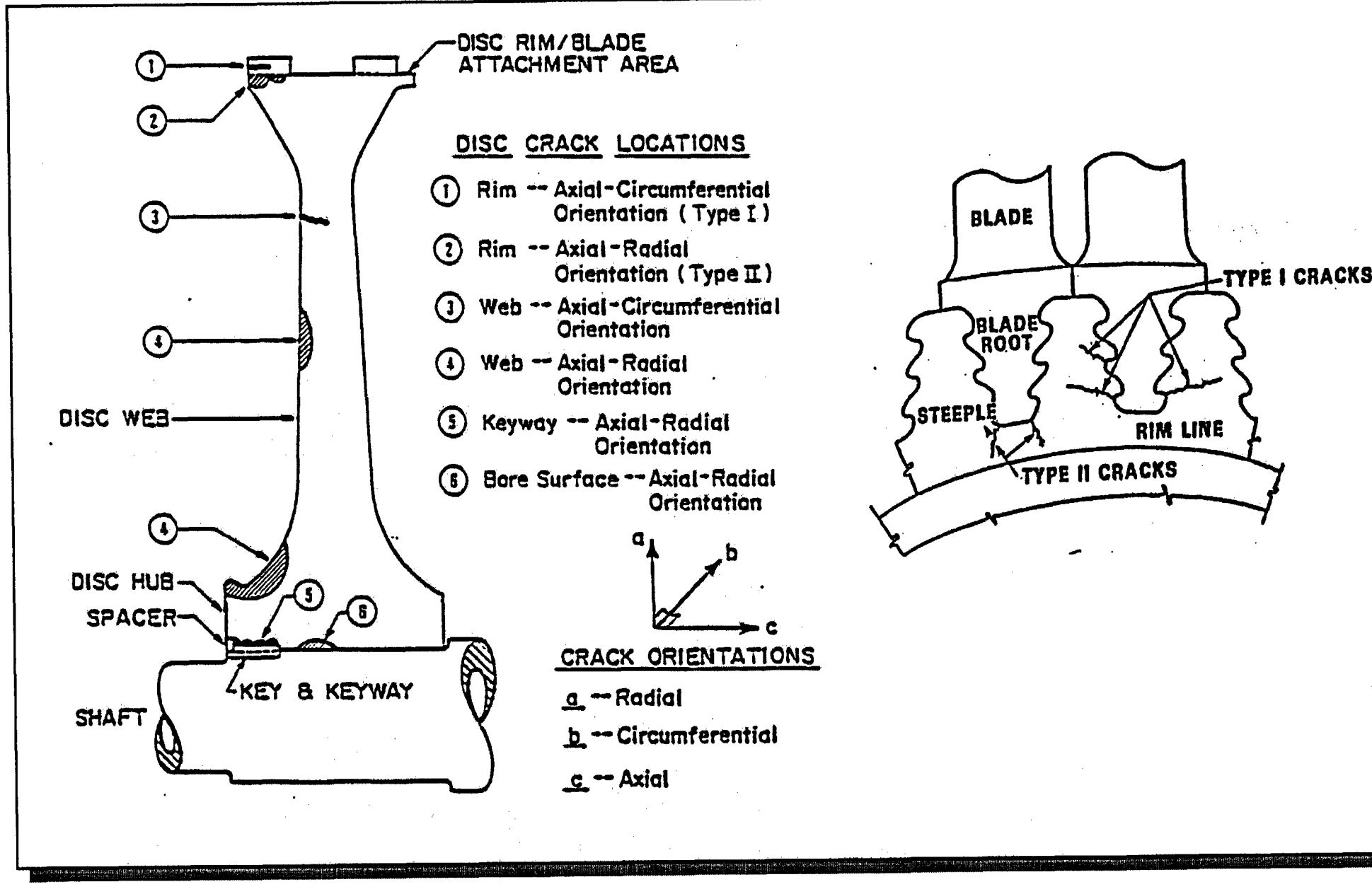

Fig. 1: SCC Problems published in the past [2]

Shrunk-on Disk Rotor

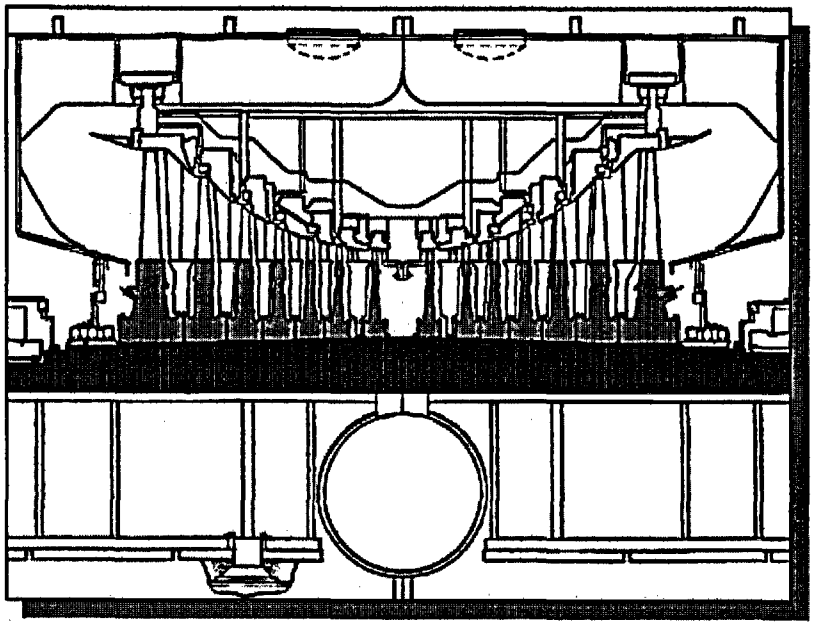

Welded Disk Rotor

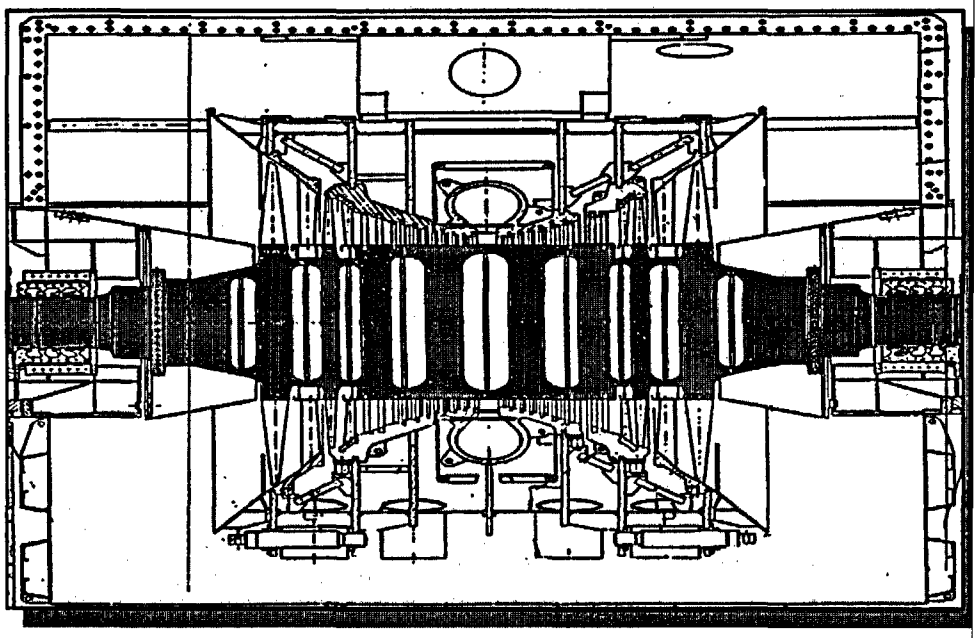

Monoblock Rotor

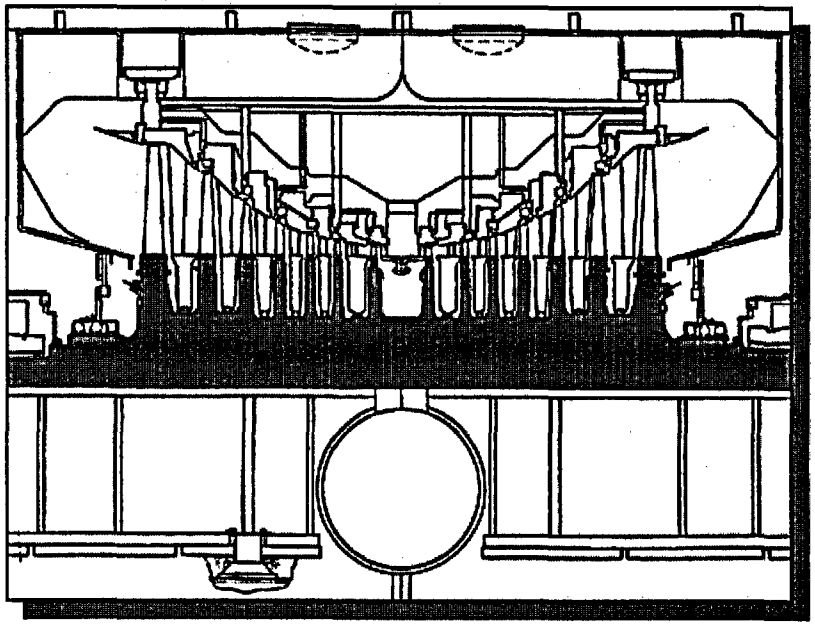

Fig. 2: Advanced Disk Rotors Replace Various Rotor Designs

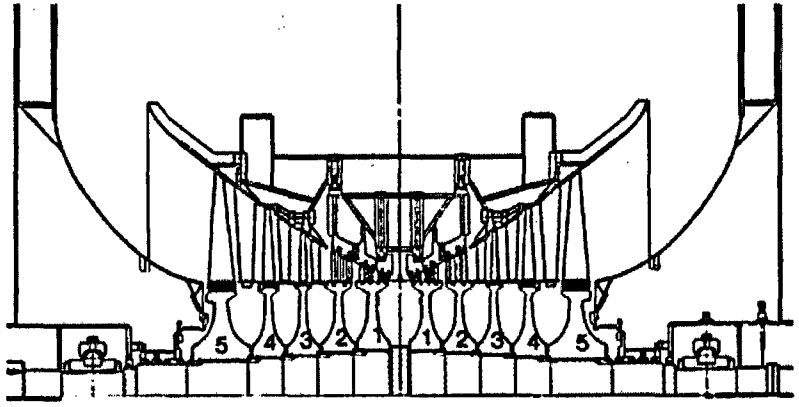

Ten-Disk Rotor – Since 1968

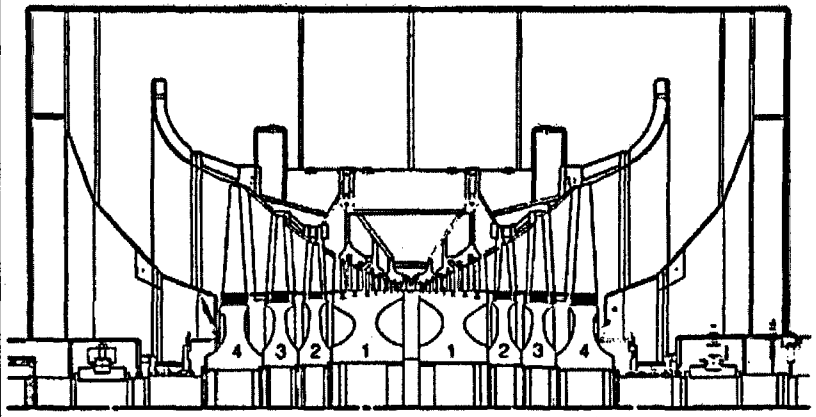

Eight-Disk Rotor – Since 1987

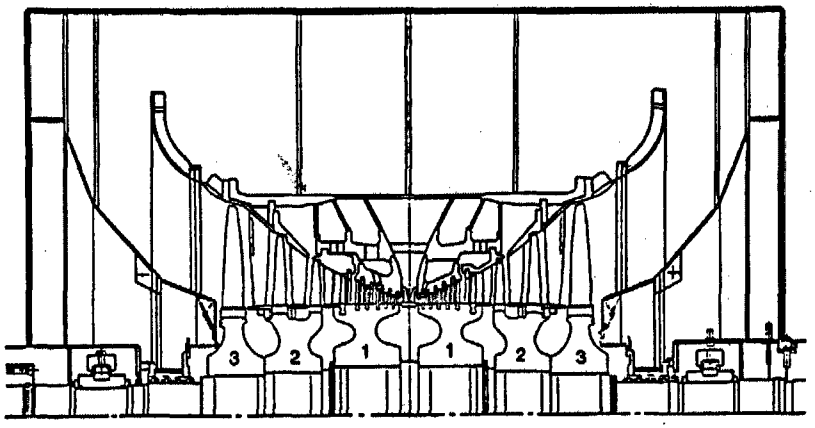

Six-Disk Rotor – Since 1995

Fig. 3: Development of Disk Rotors

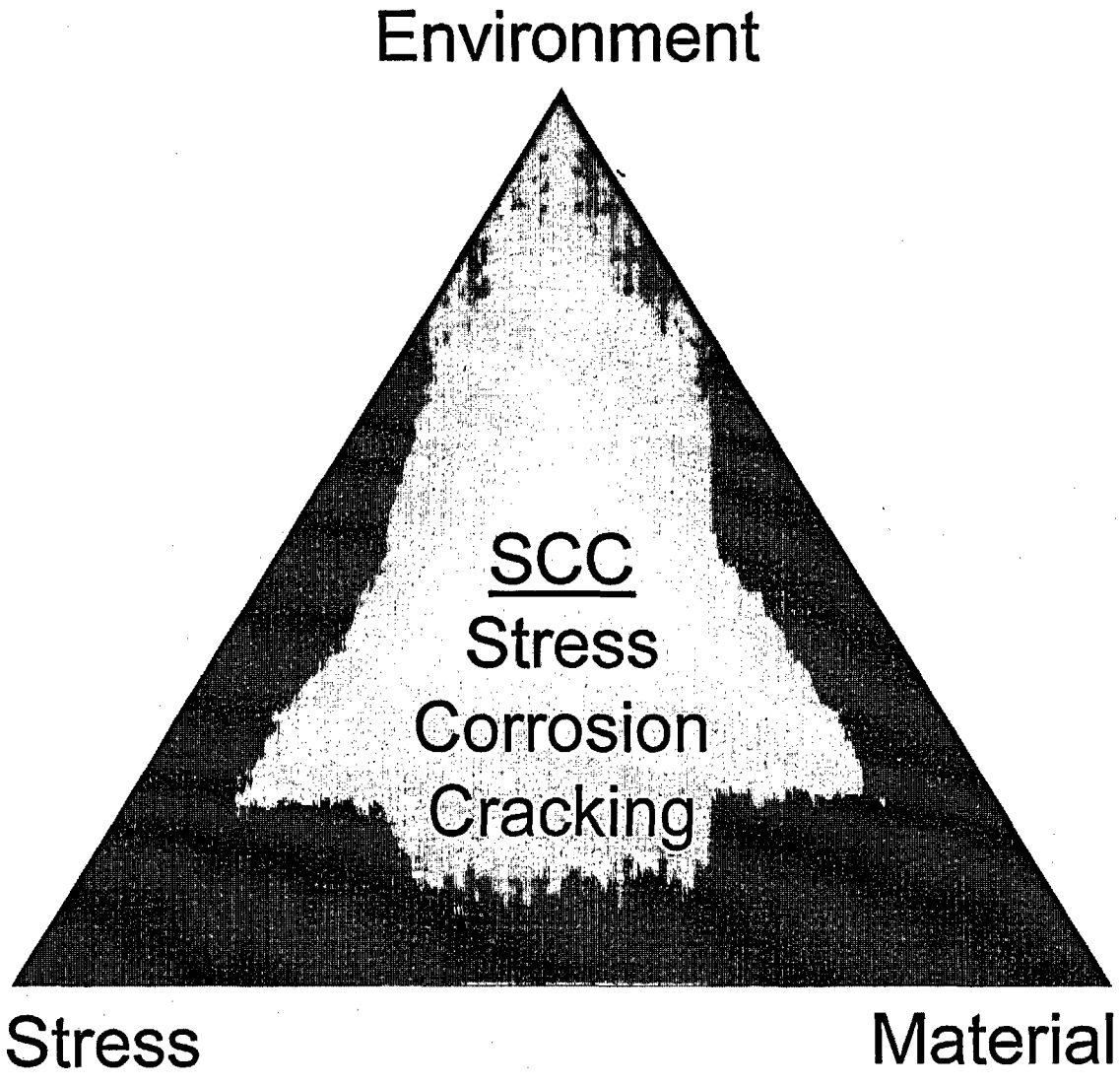

Siemens Measures

- Low Yield Strength Material
- Lower Operating Stresses
- Compressive Residual Stresses
- Lower Stress Concentrations

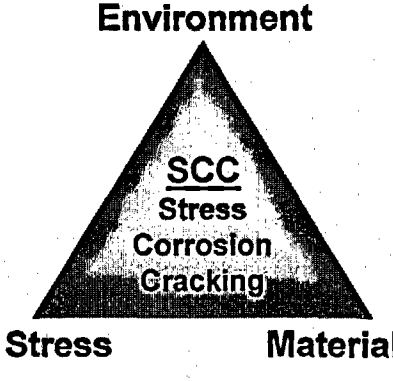

Fig. 4: Stress Corrosion Cracking (SCC) and Prevention

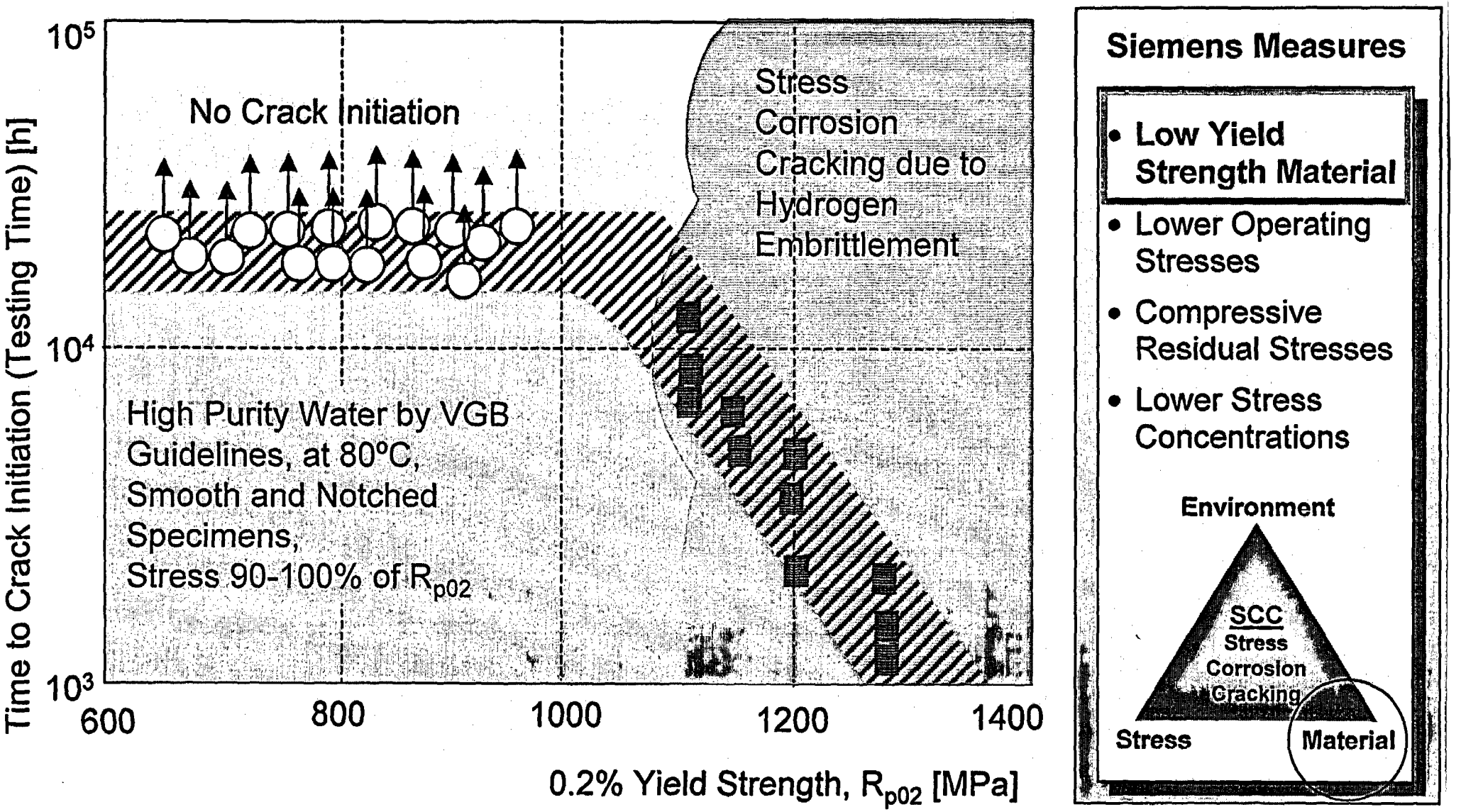

Fig. 5: Influence of Yield strength on Stress Corrosion Crack Initiation

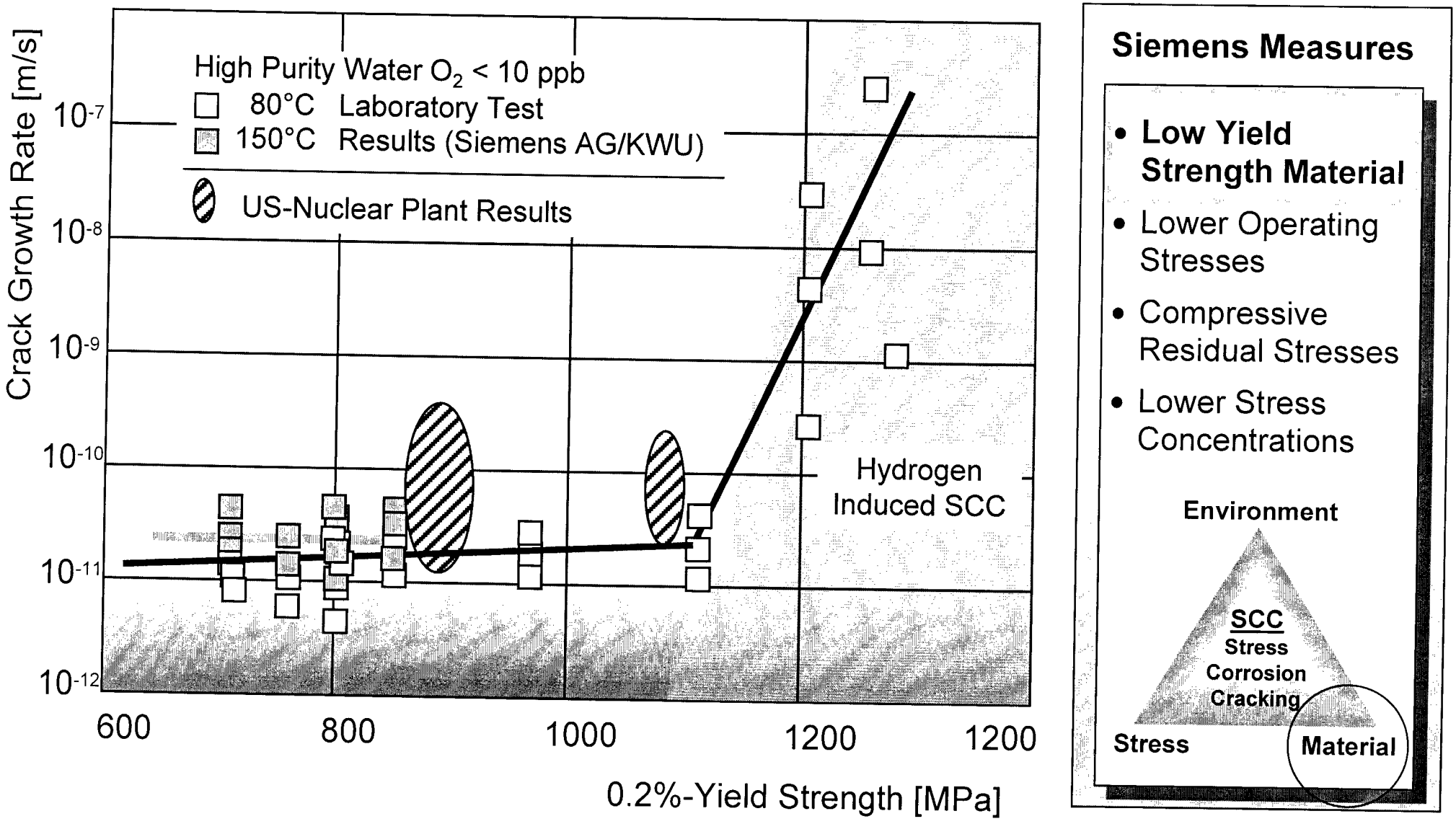

Fig. 6: Influence of Yield Strength on Stress Corrosion Crack Growth Rate

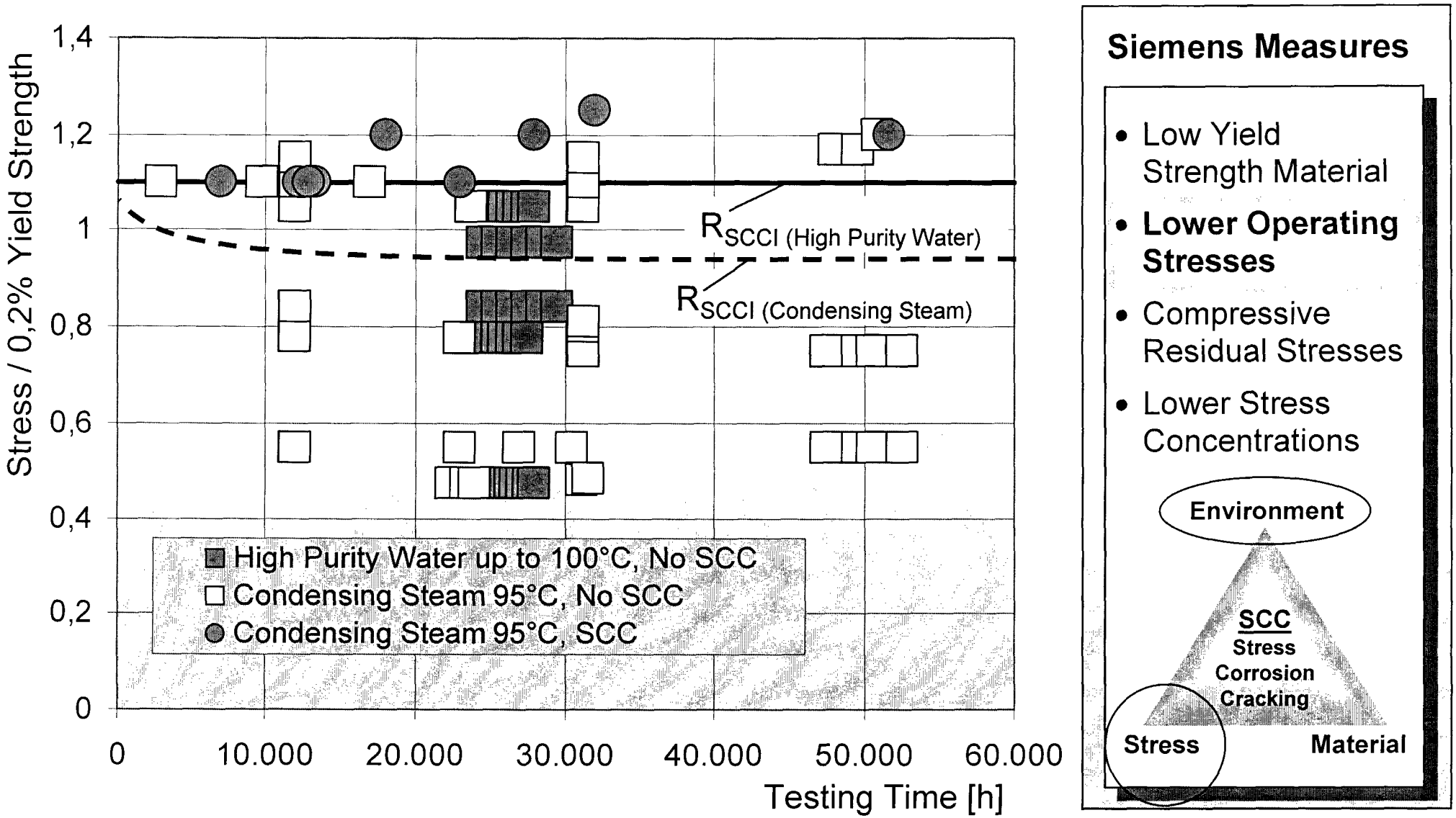

Fig. 7: Stress Corrosion Crack Initiation Tests on Turbine Disk Steels, 0.2%-Yield Strength < 1.000 MPa

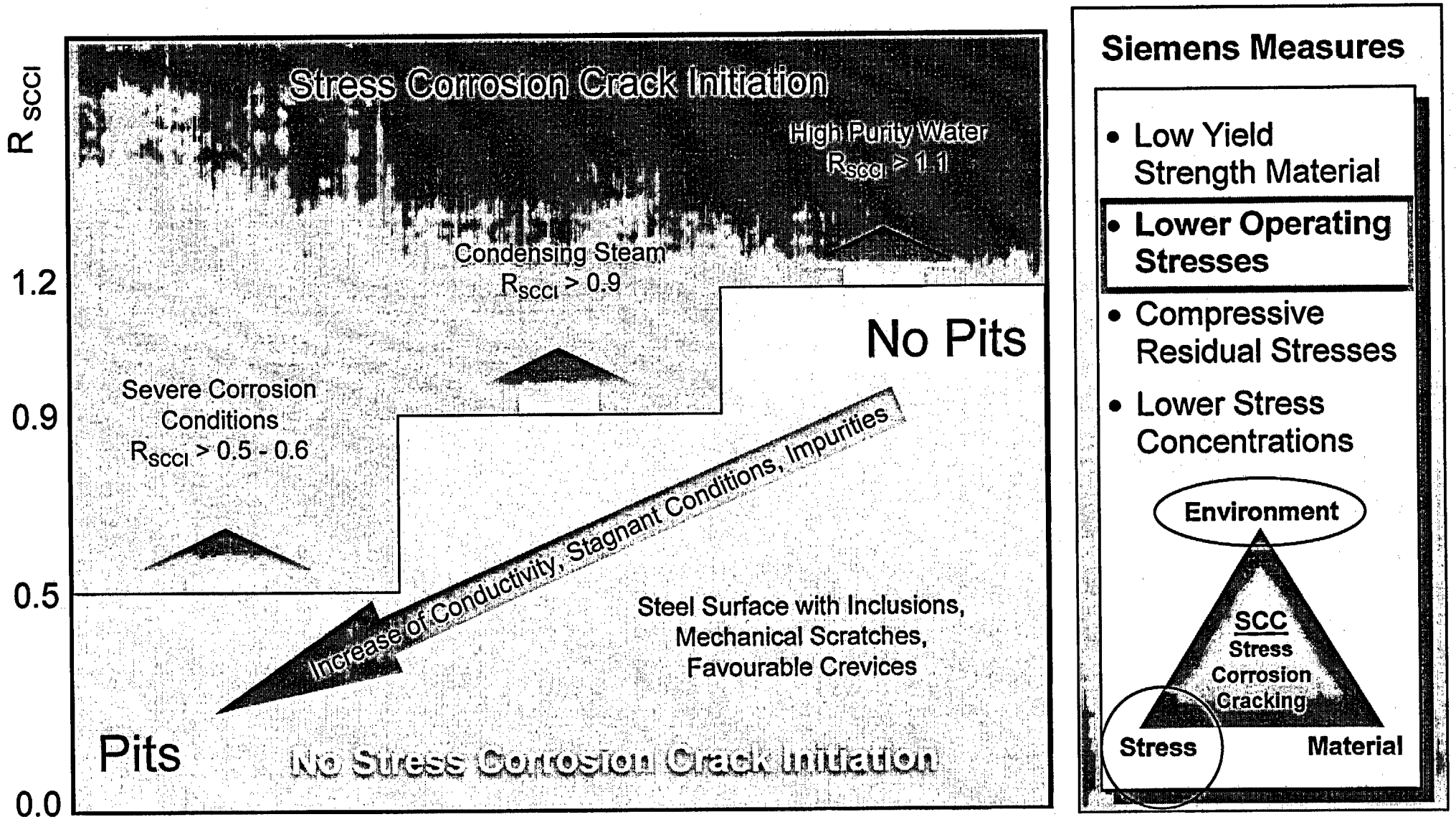

Fig. 8: Stress Corrosion Crack Initiation Threshold Value R_{scci} for Turbine Disk Steels, 0.2%-Yield Strength < 1.000 MPa

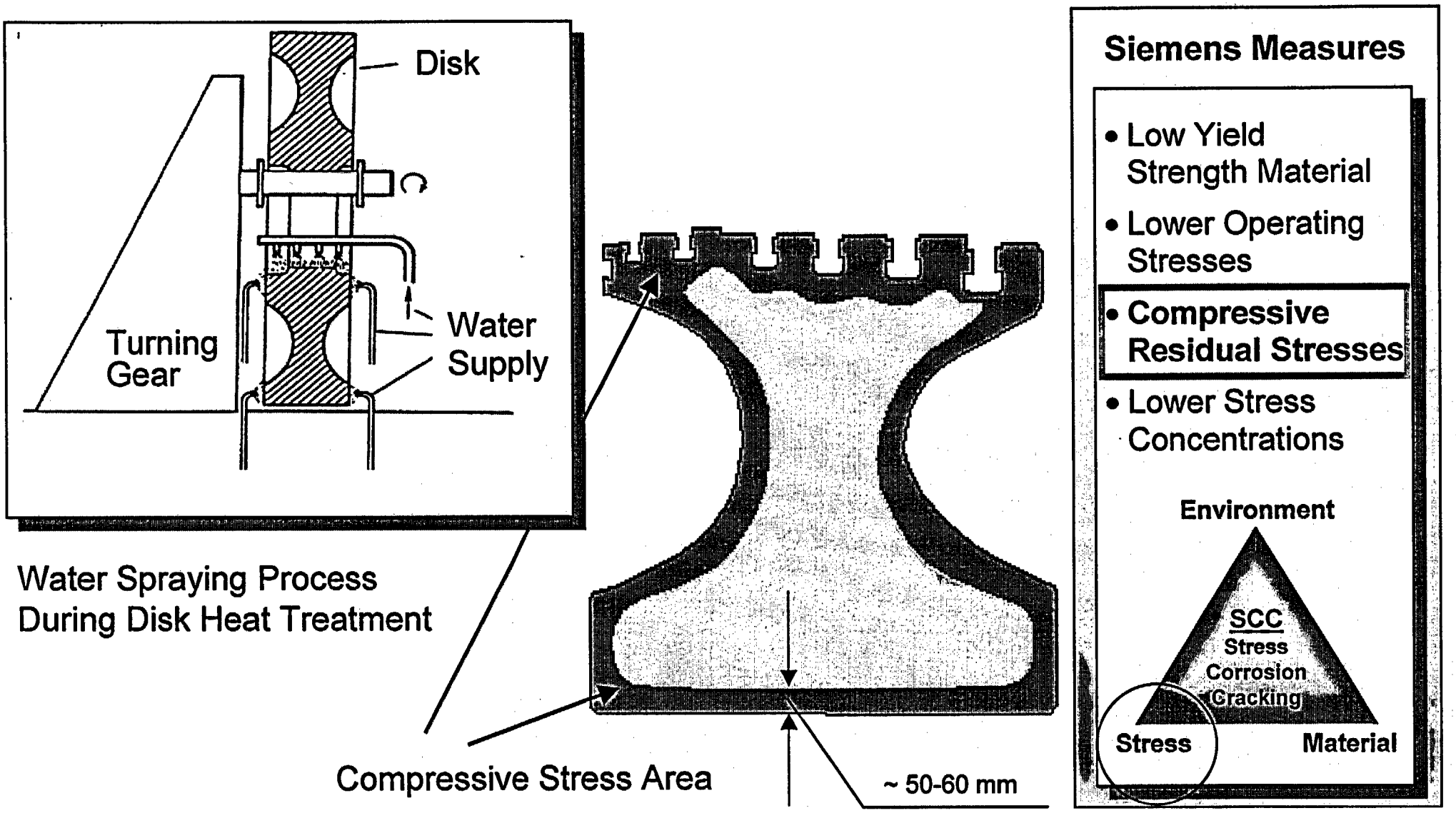

Fig. 9: Compression Residual Stresses Produced During Heat Treatment Process

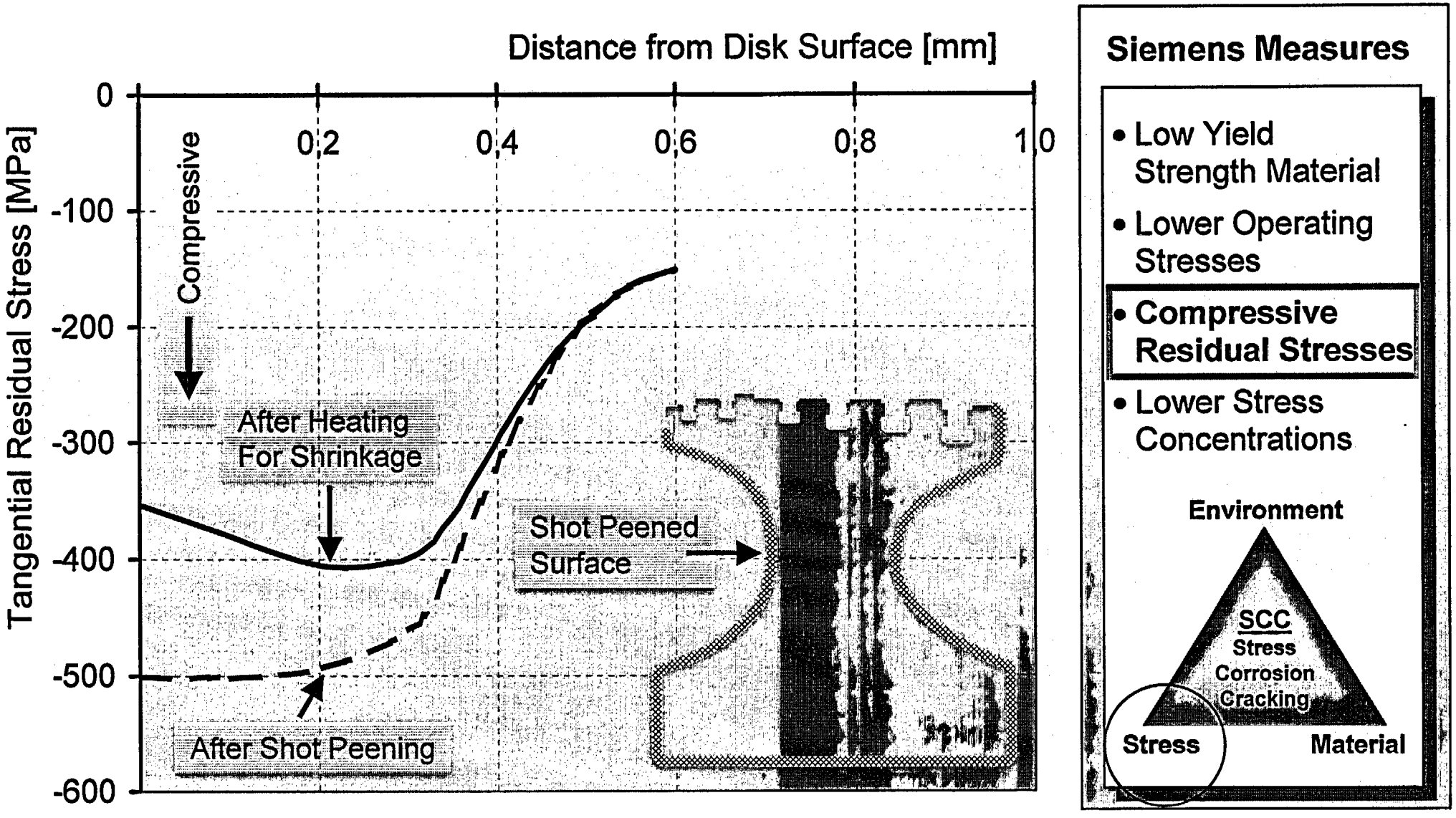

Fig. 10: Compression Residual Stresses Produced by Shot Peening Process

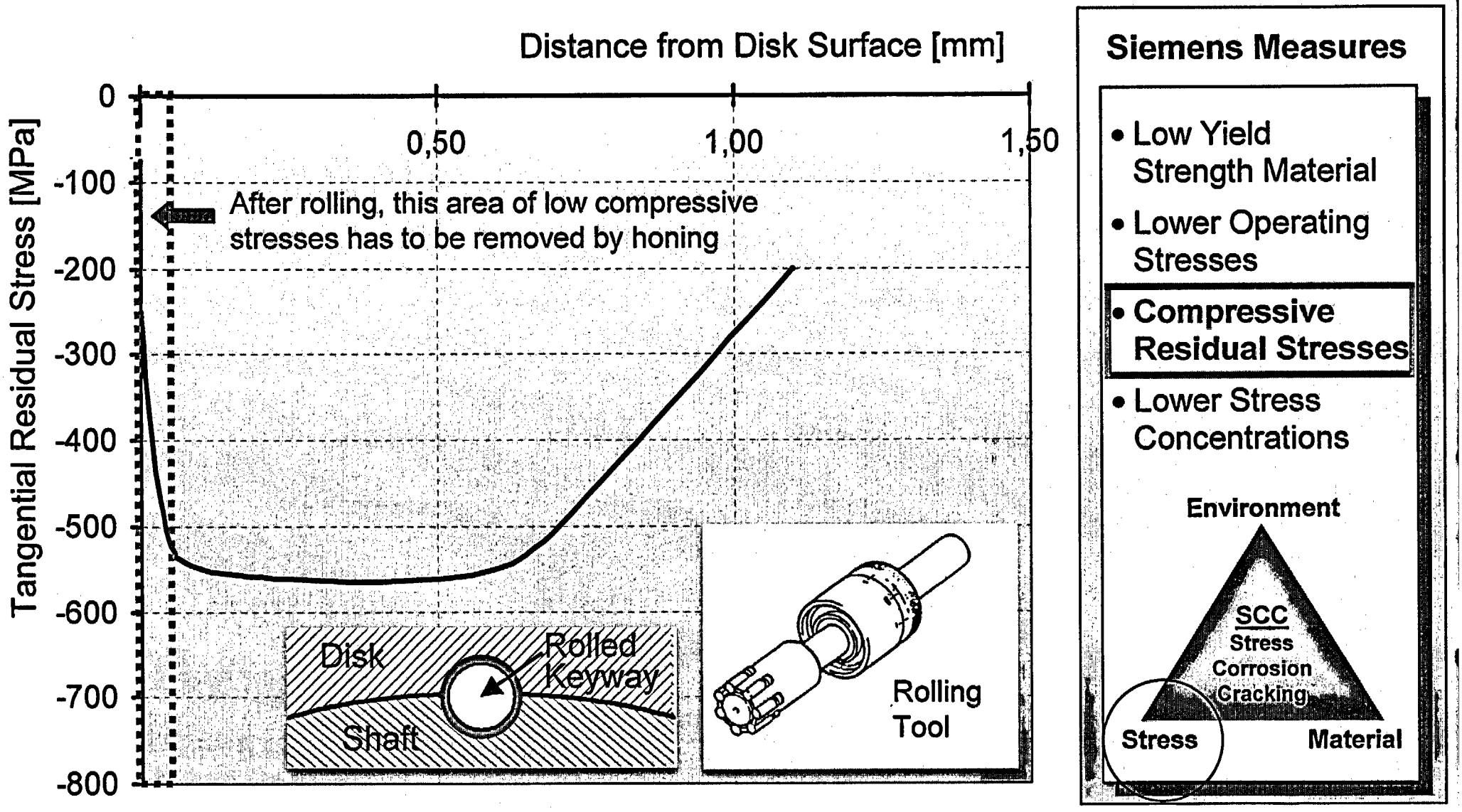

Fig. 11: Compression Residual Stresses Produced by Rolling Process

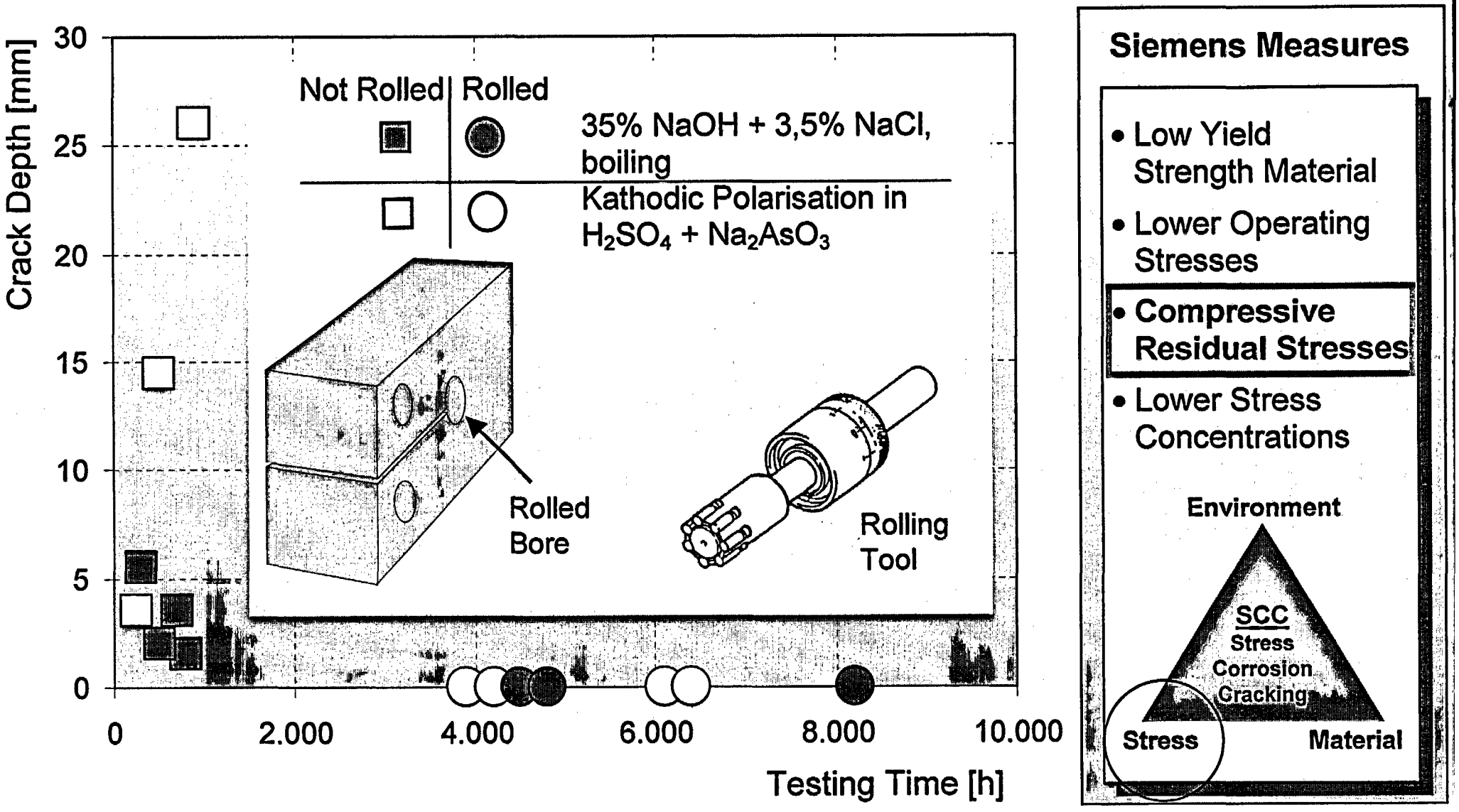

Fig. 12: Stress Corrosion Crack Initiation - Modified CT-Specimens With Residual Compression Stresses (Rolled Bore)

- No Shrink Fit Forces in Keyway Area
- Open Keyways (No Stagnant Conditions)

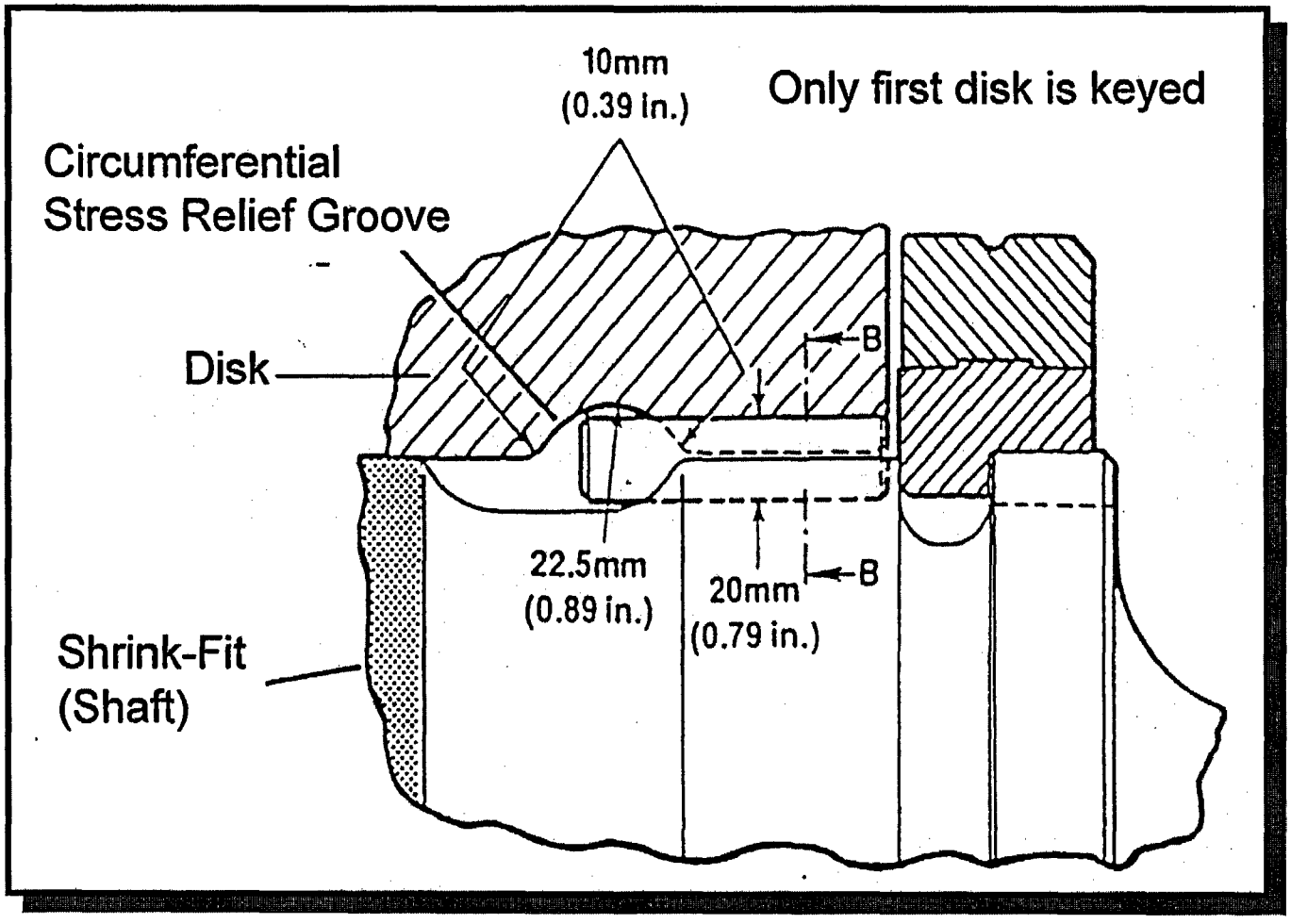

Siemens Measures

- Low Yield Strength Material
- Lower Operating Stresses
- Compressive Residual Stresses
- **Lower Stress Concentrations**

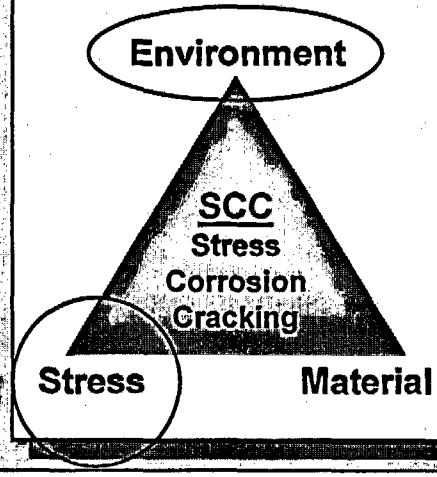

Fig. 13: Design Details from Shrink Fit and Keyway Area

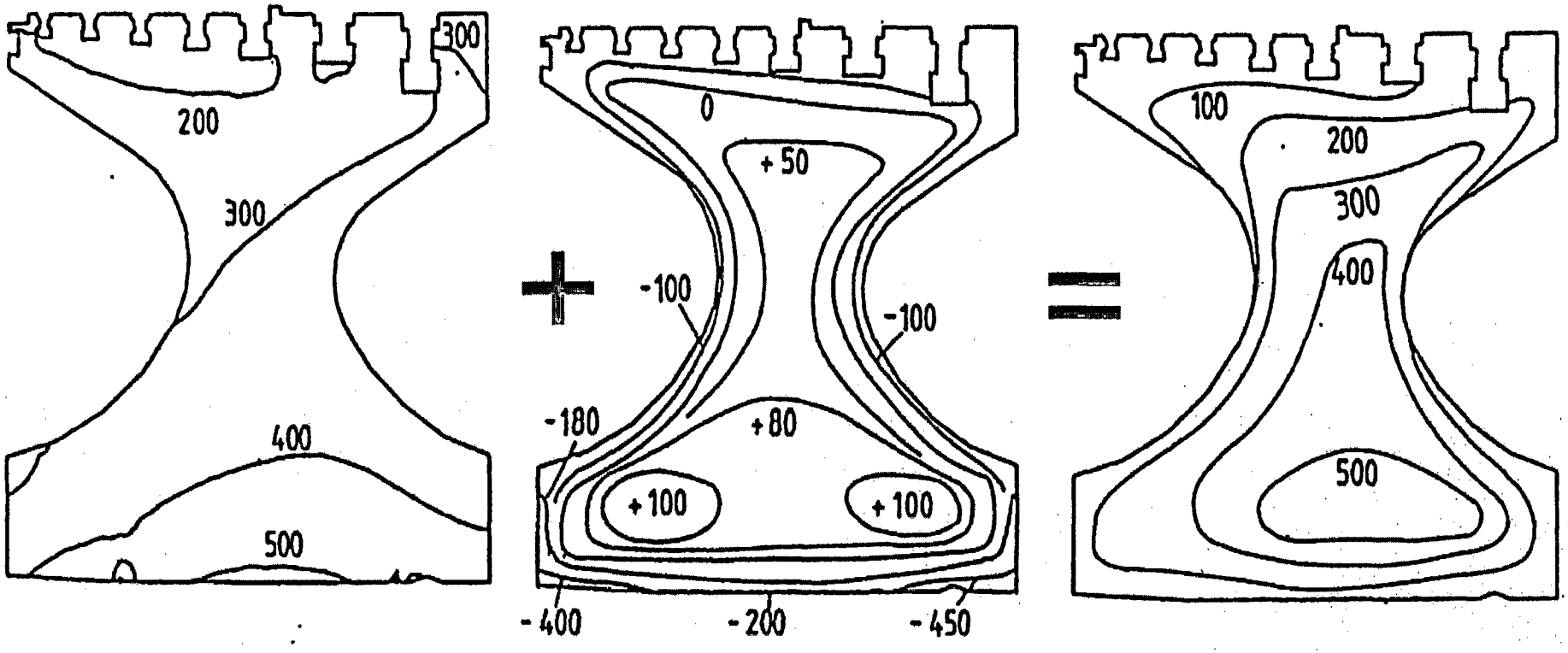

Fig. 14: Tangential Stress Distribution at Rated Speed (N/mm²)

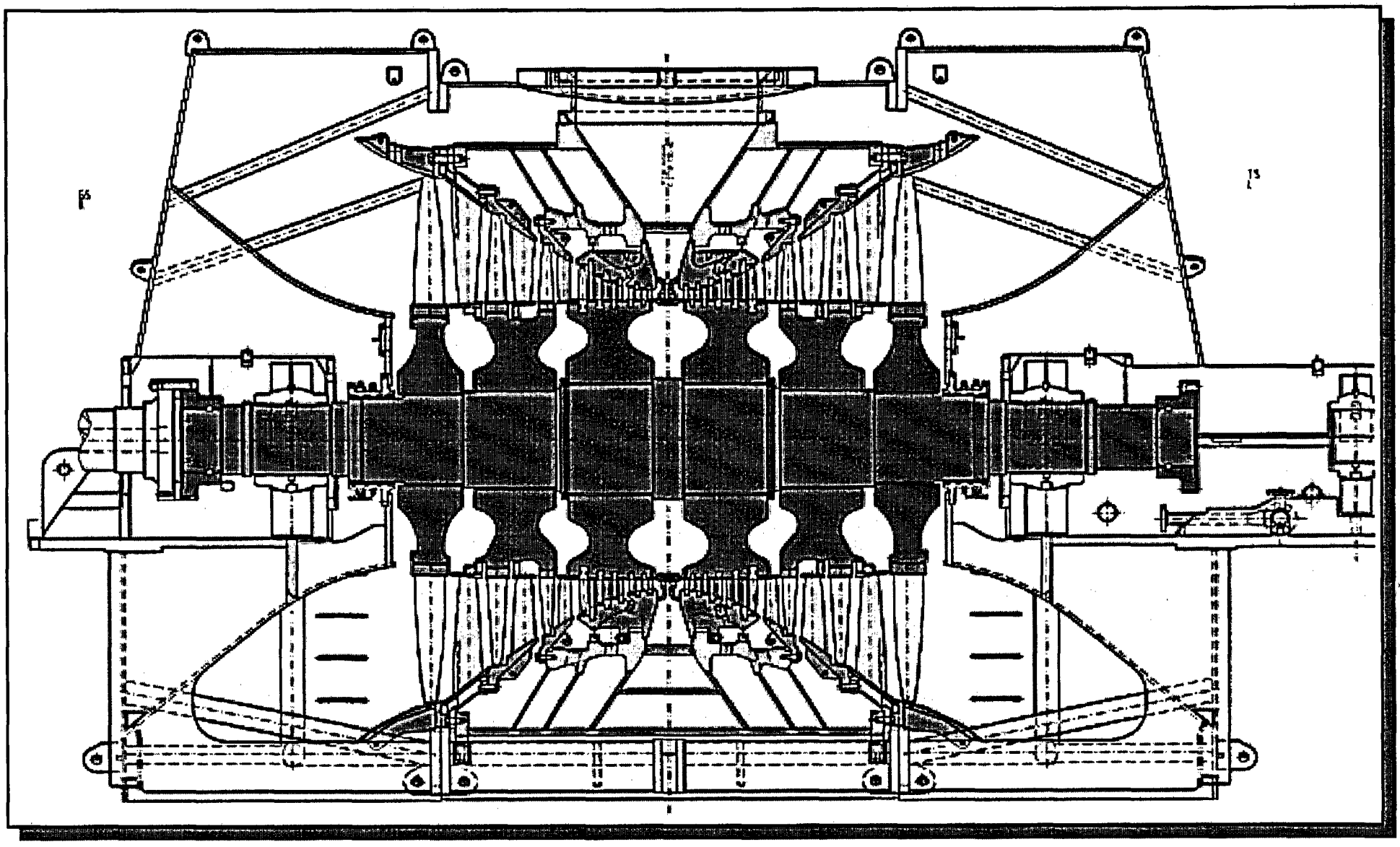

Fig. 15: Modernisation of a Westinghouse BB81/281 LP Turbine with Advanced Disk Rotors

Siemens Technical Report

CT-27332 Revision 2

Subject/Title
Missile Probability Analysis

Place	Date
Orlando, FL	8/8/2003

Author(s)	Department	Tel.	Signature
Dr. A. Bagaviev	S321	3765	
P. Bird	S326	407-736-4686	

Project
BB81/281 13.9 m^2

Signature for Release by Dept. Concerned (for Contents, Handling, Distribution)

Signature for External Release by Sales & Marketing Dept. (Not Required for Approval Documents)

Handling Instructions
Restrictive

Export Classification*) AL: ECCN:

Proj.-Code	UA or DCC	Contents Code	Doc. Ident. No.

Summary*) Pages of Text: 27 Appendices:

Missile probability analysis is presented for the Siemens 13.9m^2 retrofit design of LP turbines. These modern upgraded designs are used in various applications including replacement of Westinghouse original BB81 and BB281 nuclear LP rotors and internals.

Results of the analysis indicate that the missile probabilities remain well below the Nuclear Regulatory Commission (NRC) limits of 1E-4 for a favorably oriented unit and 1E-5 for an unfavorably oriented unit for up to 100,000 operating hours between disc inspections providing that no cracks are detected in the discs. Previously, in the submittal for the Limerick Unit [16, 17], the NRC had approved the missile analysis methodology for 10 years, which is about 87,600 operating hours. This report justifies external missile probabilities out to 100,000 operating hours in comparison with the NRC limit. Furthermore, test frequency for the main turbine stop and control valves continues at once every 3 months (quarterly), as previously approved.

*) In Technical Reports add key words (max. 12) at the end of the Summary and enter Export Classification

Distribution (add "f.i.o.", if only Summary is distributed for information):

James McCracken S326
Jim Auman S326
Andreas Feldmueller S327

Index	Vers.	Date	Page(s)	Initials of Author(s)	Initials for Release

Revisions

No.	Date	Description
0	February 26, 2003	Original issue.
1	June 6, 2003	Editorial change to add units to Figures 6 & 7.
2	August 8, 2003	Changes were made to be in full compliance with the NRC Acceptance Letter[18] and Safety Evaluation Report[19].

Contents

1 Introduction

2 Analysis Methodology

The most significant source of turbine missile is a burst-type failure of one or more bladed shrunk-on disks of the low-pressure (LP) rotors. Failures of the high-pressure (HP) and generator rotors would be contained by relatively massive and strong casings, even if failure occurred at maximum conceivable overspeed of the unit. There is a remote possibility that some minor missiles could result from the failure of couplings or portions of rotors which extend outside the casings. These missiles would be much less hazardous than the LP disk missiles, due to low mass and energy and therefore, will not be considered.

The probability of an external missile (P_1) is evaluated by conservatively considering two distinct types of LP shrunk-on disk failures, namely:

1) failure at normal operating speed up to 120% of the rated speed P_r and

2) failure due to run-away overspeed greater than 120% of rated speed P_o

for all LP disks as follows:

$$P_1 = P_r + P_o = \sum_{i=1}^{N} P_{1r} \cdot P_{2r}^i \cdot P_{3r}^i + \sum_{i=1}^{N} P_{1o} \cdot P_{2o}^i \cdot P_{3o}^i$$

where:

P_1 probability of an external missile

P_r probability of an external missile for speeds up to 120% of rated speed

P_o probability of an external missile for speeds greater that 120% of rated speed

N, i total and current number of the disks

P_{1r} probability of turbine running up to 120% of rated speed (Conservatively assumed = 1.0)

P_{2r}^i probability of disk # i burst up to 120% of rated speed due to stress corrosion crack growth to critical size

P_{3r}^i probability of casing penetration given a burst of the disk # i up to 120% of rated speed

P_{1o} probability of a run-away overspeed incident (>120% of rated speed) due to failure of overspeed protection system

P_{2o}^i probability of disk burst given run-away overspeed incident (Conservatively assumed = 1.0)

P_{3o}^{i} probability of casing penetration given a burst of the disk # i at run-away overspeed (Conservatively assumed = 1.0)

The overspeed probability P_{1o} is a function of the maintenance and test frequency of the speed control and overspeed protection system.

The probability of normal operating speeds up to 120% of the rated speed is assumed to be 1.0. It is also conservatively assumed that, given the overspeed protection system fails the probability of a disk # i burst and that of casing penetration of the burst fragments are also 1.0 each for all disks.

Finally, the expression for the external missile probability could be re-written as:

$$P_1 = P_r + P_o = \sum_{i=1}^{N} P_{2r}^{i} \cdot P_{3r}^{i} + P_{1o}$$

Therefore, the only remaining values that need to be quantified are P_{2r}^{i}, P_{3r}^{i} and P_{1o}.

The methodology for evaluation these probabilities is described in the following sections.

2.1 NRC Criteria for Missile Probability

The US Nuclear Regulatory Commission (NRC) has defined criteria governing nuclear steam turbine start-up, continued operation and shut down requirements.

Two power plant layouts, namely unfavorable and favorable orientations, have been identified as shown in Fig. 1.

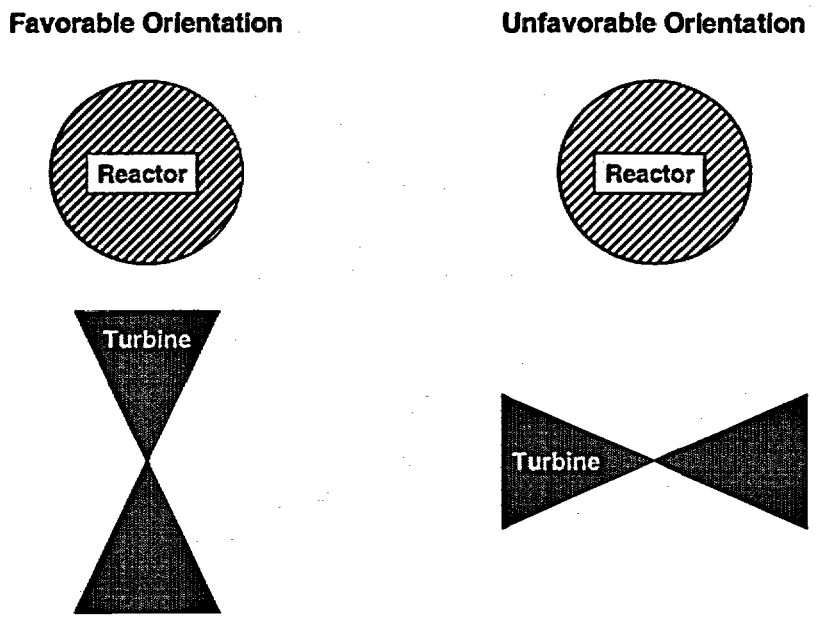

Fig. 1 Nuclear turbine unit orientation relative to reactor building

Table 1 shows the allowable limits for the probability of external missile from the steam turbine – generator unit (P_1) for start-up and continued operation. The overspeed protection system test with maintenance frequencies and disk inspection intervals must be selected to ensure that these criteria are satisfied.

Favorably Oriented Turbine	Unfavorably Oriented Turbine	Required Licensee Action
(A) $P_1 < 10^{-4}$	$P_1 < 10^{-5}$	This is general, minimum reliability requirement for loading the turbine and bringing the system on line
(B) $10^{-4} < P_1 < 10^{-3}$	$10^{-5} < P_1 < 10^{-4}$	If this condition is reached during operation, the turbine may be kept in service until the next scheduled outage, at which time the licensee is to take action to reduce P_1 to meet the appropriate A criterion before returning the turbine to service
(C) $10^{-3} < P_1 < 10^{-2}$	$10^{-4} < P_1 < 10^{-3}$	If this condition is reached during operation, the turbine is to be isolated from the steam supply within 60 days, at which time the licensee is to take action to reduce P_1 to meet the appropriate A criterion before returning the turbine to service
(D) $10^{-2} < P_1$	$10^{-3} < P_1$	If this condition is reached during operation, the turbine is to be isolated from the steam supply within 6 days, at which time the licensee is to take action to reduce P_1 to meet the appropriate A criterion before returning the turbine to service

Table 1 Turbine System reliability Criteria (NRC GUIDE NUREG-1048 Table U1)

3 Integrity Analysis

3.1 Stress Corrosion Cracking (SCC)

When materials such as used in turbine disks (Fig. 2) are exposed to sustained high tensile stress and an aggressive moist environment, cracks initiate and grow with time.

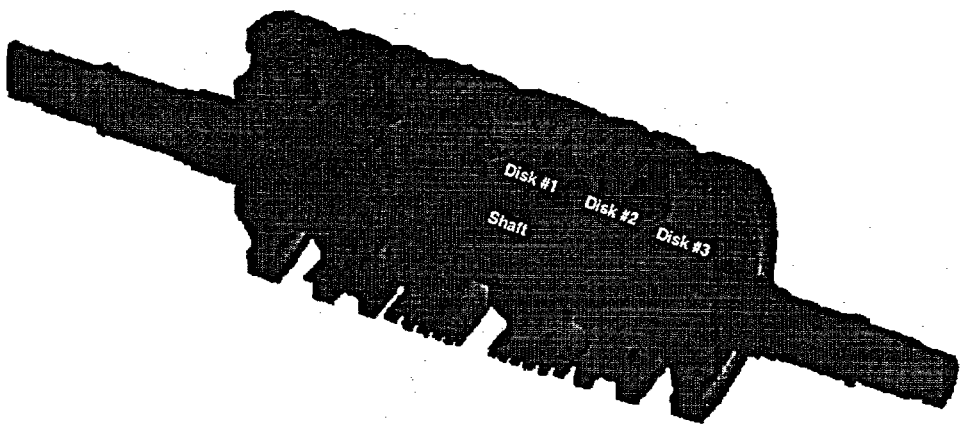

Fig. 2 Rotor with shrunk-on disks

This phenomenon is known as Stress Corrosion Cracking (SCC). Low pressure steam turbine shrunk-on disks with high stresses at the bore are susceptible to stress corrosion cracking. As a crack initiates and then grows with operating time, the stress intensity factor associated with the crack also increases. Finally, when the stress intensity factor approaches and equals the critical stress intensity factor for the material which is the fracture toughness property, a disk burst condition occurs. Alternatively, a critical crack corresponding to the material fracture toughness is calculated, and a burst condition is considered to occur when the crack size approaches and equals the critical crack size.

Siemens has conducted extensive studies into the SCC behavior of materials used for rotor disks. The results of the investigations can be summarized as follows.

SCC consists of an initial crack initiation period in which pitting or cracks are formed which is followed by a crack growth period.

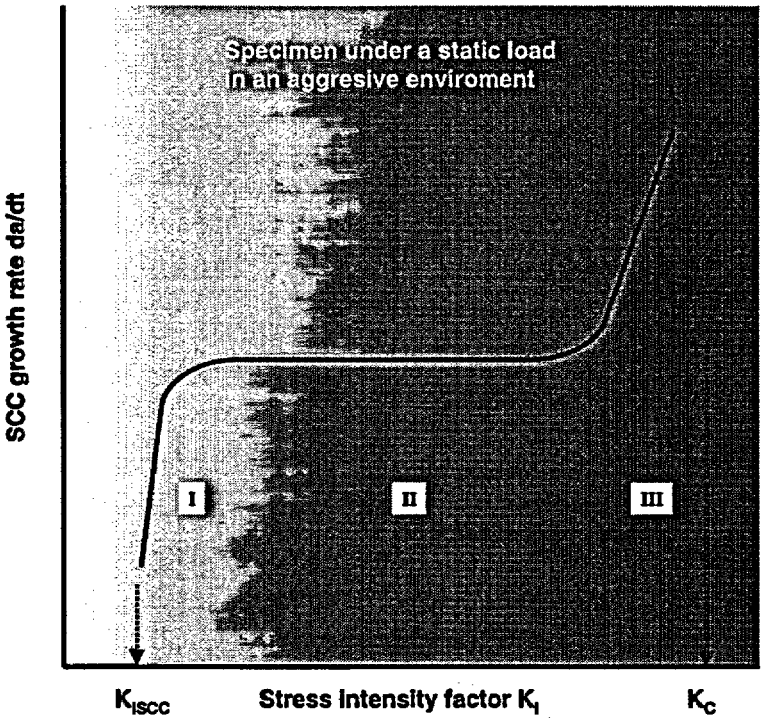

Fig. 3 Schematic dependency SCC growth rate versus stress intensity factor

Fig. 3 shows schematically the SCC growth rate as a function of the applied stress intensity factor K_I, which exhibits three distinct regions. Region I shows that no crack growth occurs below a threshold value of K_{ISCC} (typically of the order of about 20-30 MPa·√m). During region II SCC growth rate is virtually independent of the stress intensity level, until K_I approaches the material fracture toughness level. Then in region III SCC growth rate increases rapidly leading to fracture.

Impurities in steam, conditions promoting flow stagnation such as crevices, steam condensation, ratio of stress to yield strength and level of yield strength significantly influence the potential for SCC.

In high purity water with a conductivity of < 0.2µS/cm, SCC initiation is influenced only by the quenching and tempering process which establishes the material's yield strength value. If the yield strength exceeds approximately 1085 MPa (157 ksi), the material becomes susceptible to SCC due to hydrogen embrittlement. Up to this threshold, no stress corrosion crack initiation occurred even when operating stress exceeded the yield strength in notched specimens. This result is also not affected by the purity of steel. Under high purity water conditions, even nonmetallic inclusions (e.g. Al_2O_3, MnS etc.) do not act as crack starters at the material surface. Such inclusions do not influence the resistance to stress corrosion cracking. This even applies to water with low oxygen content as well as to oxygen saturated water. Pit formation was also not found under these corrosive conditions.

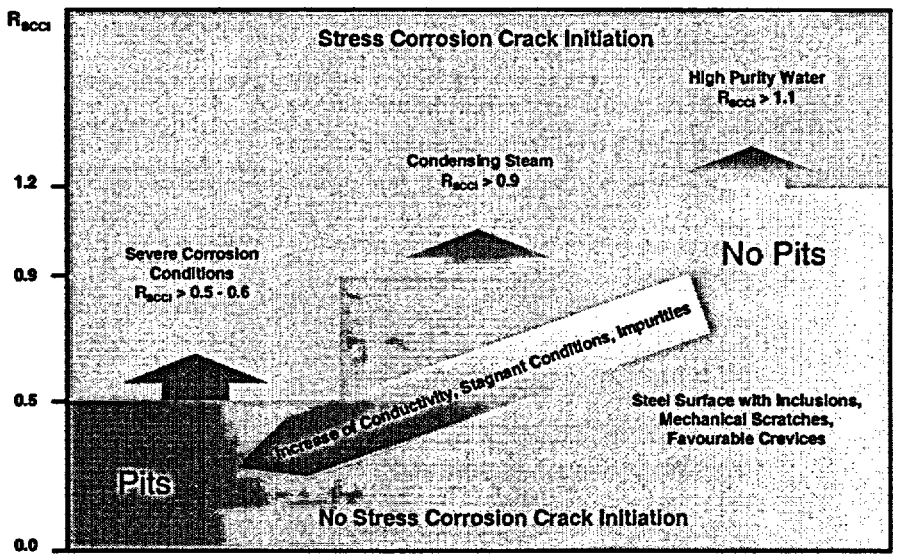

Fig. 4 Stress corrosion crack initiation of LP turbine rotor steels with 0.2% offset yield strengths < 1000 MPa (145 ksi)

Findings from extensive testing, power plant experience and review of literature leads to Fig. 4. For yield strengths less than 1000 MPa, this figure shows at what operating stress to yield strength ratios, stress corrosion crack initiation can be expected for specific environment conditions. As shown in the figure, an improvement of the operating environment permits high stress levels up to and above the yield strength level of the material. The diagram also reveals that with stress levels below 60% of the yield strength, stress corrosion cracking has not occurred even under severe corrosion conditions.

3.2 Failure Assessment Procedure

Because of the large disk bore diameter, defects on the bore surface can be treated using the basic fracture mechanics model for the case of a semi-elliptical surface crack in an infinite plate subjected to tension loading σ_{eff}. This leads to the expression for the critical crack size a_{crit} at which a disk would rupture due to brittle fracture (within the "small scale yielding" approach) given by:

$$a_{crit} = \frac{Q}{1.21 \cdot \pi} \cdot \left(\frac{K_{Ic}}{\sigma_{eff}} \right)^2 ,$$

where:

K_{Ic} = Fracture toughness,

σ_{eff} = Effective tangential bore stress due to the combined action of centrifugal loads and residual compressive stresses (manufacturing) corresponding to the Fig.5.

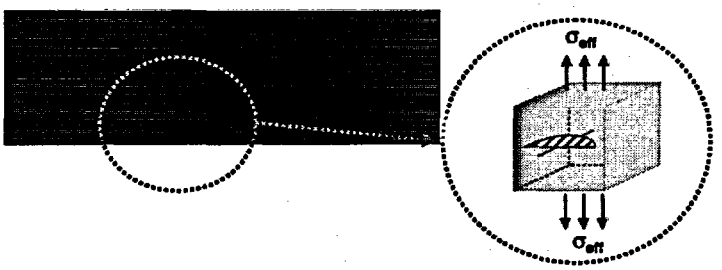

Fig. 5 Fracture mechanics model

The crack shape parameter Q is a combination of the square of the complete elliptical integral of the second kind and "small scale yielding" correction:

$$Q = E(k)^2 - 0.212\left(\frac{\sigma}{\sigma_Y}\right)^2$$

It can be for computational reasons approximated by the expression:

$$Q = 1 + 1.464 \cdot \left(\frac{a}{c}\right)^{1.65} - 0.212 \cdot \left(\frac{\sigma}{\sigma_Y}\right)^2$$

3.3 Stress Analysis

The finite element analysis of the rotor with the shrunk-on disks (Fig. 2) was conducted to determine the temperature and stress distribution due to the combined effect of shrink fit, thermal and centrifugal mechanical loads. The disk material is 26NiCrMoV14-5.

Temperature (Fig. 6) and tangential stress (Fig. 7) distributions in the disks are computed using a commercial Finite Element Code ABAQUS [9]. All appropriate loading conditions must be considered in order to obtain the appropriate stress distributions for input to the fracture mechanics evaluation in the location of interest.

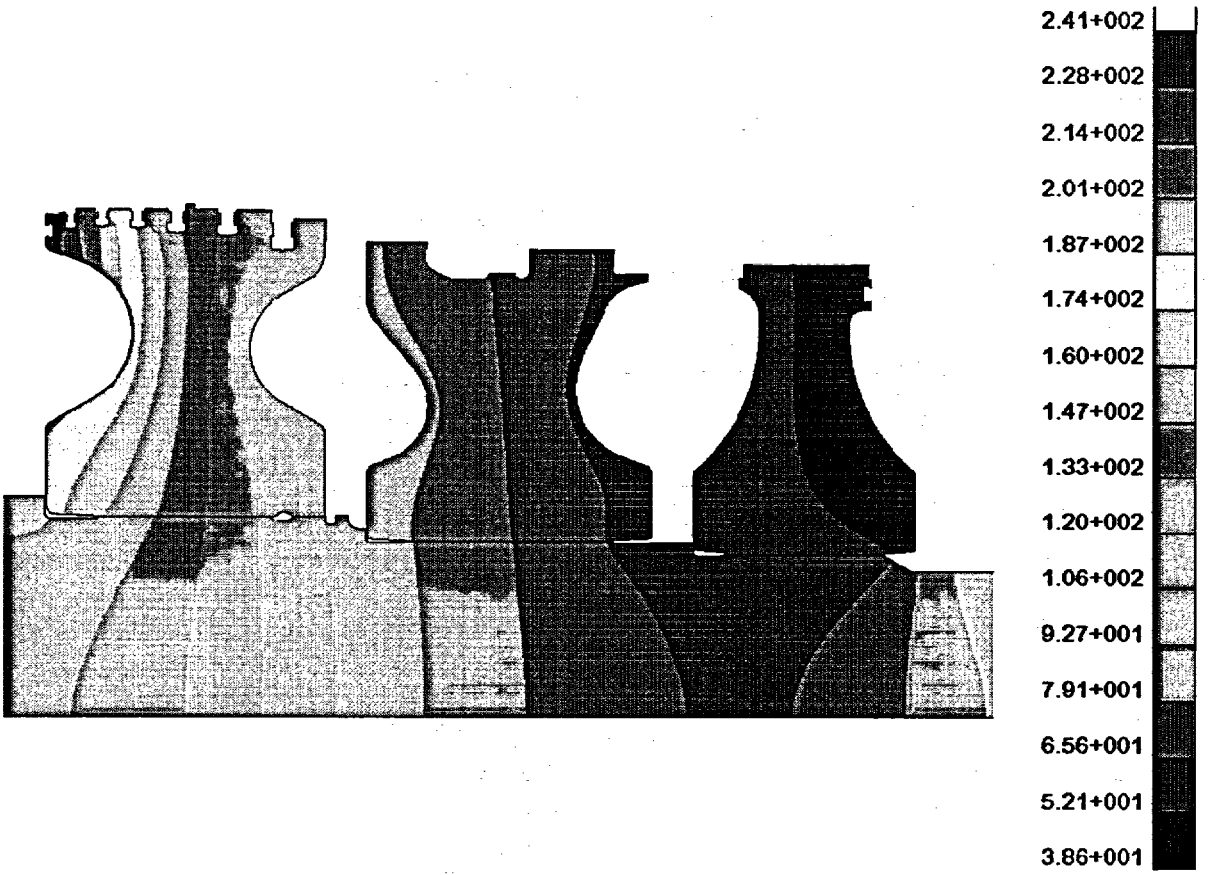

Fig. 6 Temperature distribution
(Units In Degrees C)

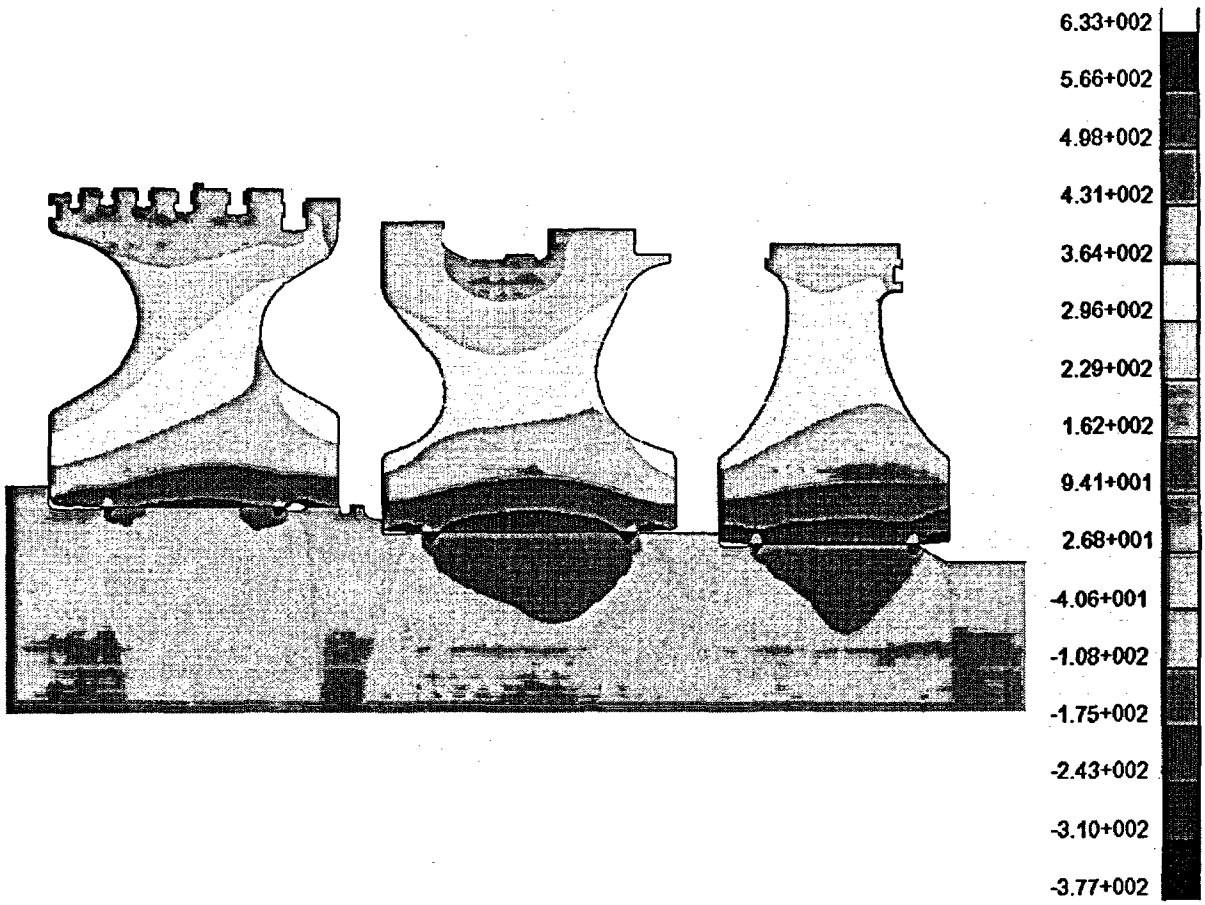

Fig. 7 Tangential stress distribution
(Units in MPa)

Fig. 8 shows schematically the blue-colored compressive stress region (the width about 50 mm) and red-colored tensile stress region in the disk after special heat treatment during manufacturing. The corresponding distribution of the residual stress is presented as a brown line. The tangential stress distribution at 20% overspeed near the disk bore at the maximal stress location is shown as a red line. The combined effective stress distribution is presented as a dashed blue line.

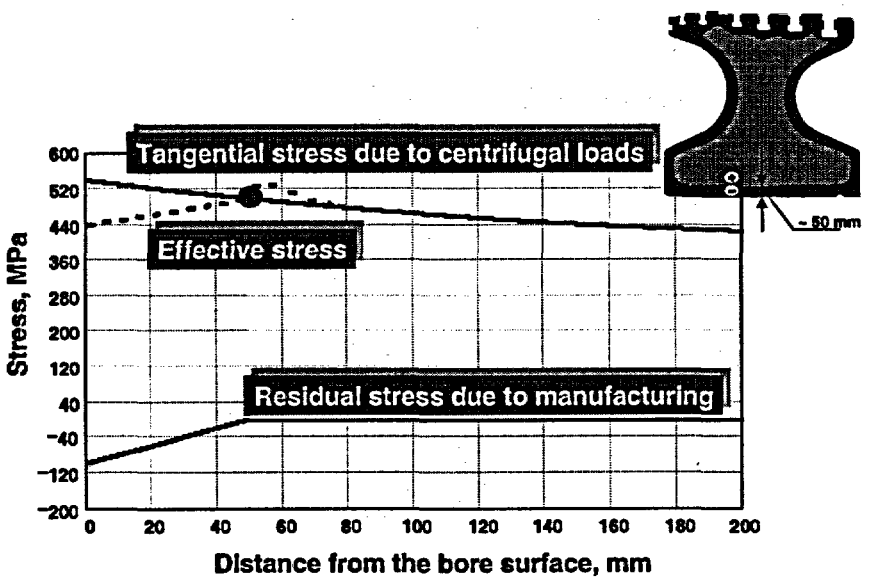

Fig. 8 Tangential (at 120% of rated speed), residual and effective stress distribution in the disk #1

3.4 Probabilistic Fracture Mechanics Analysis

For probabilistic computations, Siemens has developed a numerical Monte-Carlo simulation code. As a failure condition the brittle fracture mode is assumed:

$$a_{cr}(K_{Ic}, \sigma_Y, \sigma, \xi, k) \le a_i + \int_0^t \dot{a}(\sigma_Y, T)\,dt\,.$$

Where:

a_{cr} = Critical crack size,

a = Current crack size,

a_i = Initial crack size,

t = Operating time duration,

ξ = Crack shape factor (crack depth to crack length ratio),

K_{Ic} = Fracture toughness,

k = Branching factor,

σ = Applied load due to tangential stress at bore,

σ_Y = Yield strength, and

T = Temperature.

For probabilistic analysis the critical crack size is defined as that given by the equation in Section 3.2 or 100 mm whichever is smaller. The 100-mm limit is purely based on the applicability limitation of linear-elastic fracture mechanics concept and does not necessarily represent an imminent burst condition.

A brief description of selected random variables is given below.

3.4.1 Load

It is assumed that FE Analysis provides accurate results within 5% of tolerance due to the uncertainties in geometry as well as thermal and mechanical loads. A normal distribution is assumed. The mean values are shown in Table 2.

	Disk # 1	Disk # 2	Disk # 3
Metal temperature [ºC]	130	80	57
Tangential stress [MPa]	498	521	535

Table 2 FE computation results

3.4.2 Crack Branching Factor

The branching factor k is assumed to be normally distributed with a mean of 0.65 and a standard deviation of 0.175, whereby

$$k = \begin{cases} 0.65 \; if \; Crack\,Depth \leq 3\,in \\ 1 \quad otherwise \end{cases}$$

3.4.3 Fracture Toughness

The normal distribution has been used in describing scatter in fracture toughness data with a mean of 219.8 MPa$\cdot\sqrt{m}$ and standard deviation of 10% of the mean value.

3.4.4 Yield Strength

The yield strength values are assumed to be distributed normally with mean and standard deviation values based on internal investigation data:

Disk # 1: σ_Y = 815 MPa and std. deviation = 30 MPa

Disk # 2 and 3: σ_Y = 855 MPa and std. deviation = 30 MPa

3.4.5 SCC Growth Rate

As shown in Fig. 3 the stress corrosion cracking (SCC) rate is assumed to be independent on the stress intensity level. The main parameters influencing the SCC rate are temperature, material yield strength and water chemistry. Based on field measurements and laboratory test data the empirical equations for SCC rates were developed. For the probabilistic analysis the Westinghouse SCC rate is used:

$$\frac{da}{dt} = \exp(-4.968 - \frac{7302}{T + 460} + 0.0278 \cdot \sigma_Y),$$

Where the SCC rate is given in inches/hour, temperature T in ºF and the material yield strength σ_Y in ksi.

The log-normal distribution of Westinghouse-SCC rate with a standard deviation of 0.578 is assumed.

3.4.6 Initial Crack Size

The initial crack size is assumed to be a non-varying variable with the value a_i = 3 mm.

3.4.7 SCC Initiation Model

Since SCC initiation is not understood well enough to be quantifiable as a function of time, it is modeled based on the observed cracking experience of the turbine disks in the field.

3.4.7.1 „Old" Approach

To date a total of 82 Siemens AG PG #1 disks and 324 latter disks from 41 ten and eight disk LP rotors in operation have been inspected or re-inspected world wide over the last 20 years. Two of the newest six disk design rotors have been in operation only since September 1996 and eight more installed during 1997-99. Thus, no inspections have been made on these six disks design rotors to date. Only one #1 disk on a ten disks design rotor was found to have SCC type ultrasonic indication in the disk hub surface. There were no cracks in the higher stressed keyways. This finding was after 67,600 operating hours. This design did not have the benefit of design induced compressive residual stresses on the disk hub bore. Subsequent inspections found crack growth rate to be 3-4 mm per year. An in-

vestigation of the cause showed that the disk hub surface was contaminated by microscopic Ni-rich and S-rich particles, which were inadvertently introduced and pressed into the surface during the time of manufacture. This probably acted as the crack starter. Manufacturing procedures were redefined to preclude such occurrences in the future. Small indications were also found on two of the 324 latter disks. The nature of these indications could not be ascertained but are likely to be due to water erosion or SCC. Details of these findings have been reported earlier [11]. These two findings were on the inlet side of the TE and GE disk #4 of the same rotor. This rotor was also of ten disks design unit without induced residual stresses of the disk hub bore. The indications were found after 53,000 operating hours. Evaluation found no limitation to designed operating life, the rotor was returned to service and additional investigation to this time has not been possible due to the disks being in service.

Conservatively, assuming that all of the above indications are due to SCC and using standard statistical evaluation procedures, the crack initiation probabilities at 90% confidence level for the #1 disks are as shown in Table 2.

Disk	Crack Initiation Probability
1	$4.63 \cdot 10^{-2}$
2	$4.63 \cdot 10^{-2}$
3	$1.64 \cdot 10^{-2}$

Table 3 Crack Initiation Probability

3.4.7.2 Modern Approach

The probability of crack initiation in a given disk is estimated from the inspection data of turbine disks and the probability value depends on the disk # and the location of indication, i.e. either the keyway or hub bore. Thus, the crack initiation probability is treated as a binomial variant and estimated directly from field data showing the number of cracks found and the number of disks inspected for each disk type [10]. The probability of crack initiation in a disk # i :

$$q_i = \begin{cases} \dfrac{\text{number of \#i disks with cracks}}{\text{number of inspected \#i disks}} \\ 1-(0.5)^{1/(\text{number of inspected \#i disks})}, \text{ if the number of \#i disks with cracks} = 0 \end{cases}$$

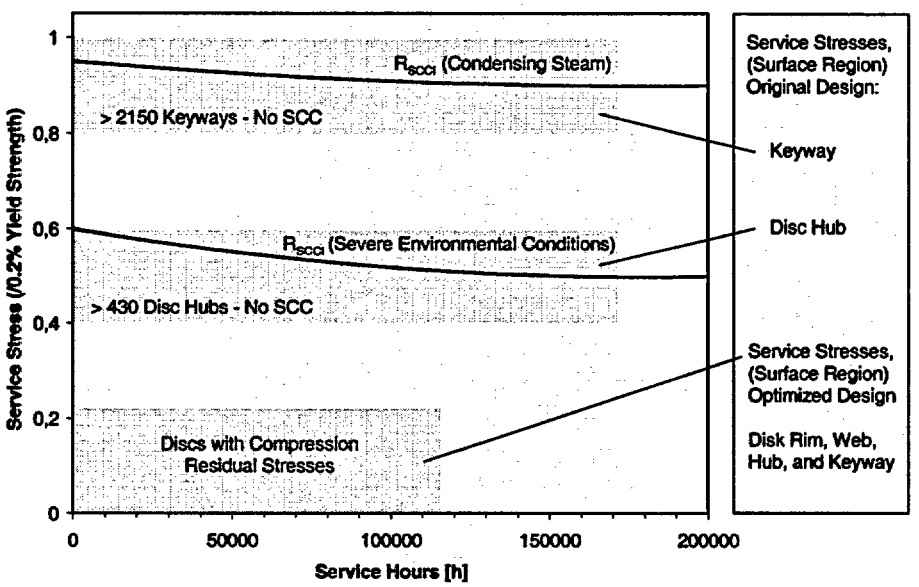

Fig. 9 Results of the investigation on crack initiation

Based on the investigation results [14,15] shown in Fig. 9 the following crack initiation probabilities q_i can be calculated:

Keyway area: $q_i = 1 \cdot 10^{-6}$ (2150 investigated keyways without any indication)

Disk hub area: $q_i = 1.6 \cdot 10^{-3}$ (more than 430 investigated disks without any indication)

For the probabilistic calculations the more conservative "old" approach is assumed.

4 Probability of Casing Penetration for Speeds up to 120% of Rated Speed

4.1 Criterion for Casing Penetration Given a Disk Burst

The criterion for an internal missile fragment penetrating the surrounding blade ring and inner and outer casing structure is stated as follows:

$$E_i \geq E_d,$$

where

E_i is the total initial energy of the internal missile due to burst;

E_d is the total energy dissipated due to various resisting factors

A generic description of the procedure is as follows:

4.1.1 Initial Energy

The size of the angular segment of the disk with the blades is determined by maximizing the translational energy of the internal missile. The total energy of the missile segment is given by

$$E_i = \frac{1}{2} \cdot I \cdot \omega_b^{\,2}$$

Where:

I = Polar moment of inertia of the missile segment;

ω_b = Rotational speed at burst.

4.1.2 Energy Dissipation

Energy dissipation factors considered include blade crushing, blade bending, loss of blade mass due to break off, friction between missile fragment and inner casing structure, deformation of the stationary blade ring and inner casing up to breakage and penetration through the outer casing structure.

4.1.3 Calculation Results

The surrounding casing is designed to prevent external missiles up to at least 120% of rated speed.

The calculated speeds at which ductile burst of disks occurs are 177%, 175% and 170% respectively for the disks # 1, # 2 and # 3.

Based on the Monte Carlo simulation technique with 10^6 calculations the probability of casing penetration at 120% rated speed was determined. The probabilities respectively are $9.0 \cdot 10^{-6}$, $6.3 \cdot 10^{-6}$ and $2.9 \cdot 10^{-5}$ assuming a friction coefficient of 0.25.

5 Overspeed Event

Run-away overspeed events (>120% of rated speed) are due to failure of the overspeed protection system which consists of speed monitoring devices, trip and fast closure of steam stop and control valves. Siemens evaluates nuclear and fossil unit control systems together due to common control components, with the older fossil units adding conservatism [2,3]. Based on the upper confidence limit

evaluations, the following overspeed probability values are used for the three typical valve test frequencies.

Valve Test Frequency	Probability of Overspeed, Yr^{-1}
Weekly	$1.6 \cdot 10^{-7}$
Monthly	$9.0 \cdot 10^{-7}$
Quarterly	$3.0 \cdot 10^{-6}$

Table 4 Overspeed probability values

For these probabilistic calculations, the probability corresponding to quarterly valve test intervals is conservatively assumed.

6 Probabilistic Simulation Results

The probabilistic results were generated using a Monte Carlo simulation technique involving successive deterministic fracture mechanics calculations using randomly selected values of variables described in the Section 4.3. One million simulations were performed for each disk. Reproducibility and consistency of results was tested using various random number generators and random number seeds.

The results of calculations are representatively shown in Table 5.

	Disk #1	Disk #2	Disk #3
P_{2ri}	$4.63 \cdot 10^{-2}$	$4.63 \cdot 10^{-2}$	$1.64 \cdot 10^{-2}$
P_{2rg}	$5.2 \cdot 10^{-2}$	$5.4 \cdot 10^{-4}$	$3.0 \cdot 10^{-5}$
$P_{2r} = P_{2ri} \cdot P_{2g}$	$2.4 \cdot 10^{-3}$	$2.5 \cdot 10^{-5}$	$4.9 \cdot 10^{-7}$
P_{3r}	$9.0 \cdot 10^{-6}$	$6.3 \cdot 10^{-6}$	$2.9 \cdot 10^{-5}$
$P_r = P_{2r} \cdot P_{3r}$	$2.2 \cdot 10^{-8}$	$1.6 \cdot 10^{-10}$	$1.4 \cdot 10^{-11}$
$\sum_{i=1}^{6} P_r$	$1.3 \cdot 10^{-7}$	$9.5 \cdot 10^{-10}$	$8.6 \cdot 10^{-11}$

Table 5 Representative calculation for the 100,000 hours inspection interval

Since $P_{1o} = 3.42 \cdot 10^{-5}$, which is $3.0 \cdot 10^{-6}$ per year for 100,000 hours, the total probability of an external missile (P_1) for the unit at 100,000 hours inspection interval is:

$$P_1 = 1.3 \cdot 10^{-7} + 3.43 \cdot 10^{-5} = 3.43 \cdot 10^{-5} < 11.42 \cdot 10^{-5} \text{ (NRC limit value for 100,000 hours)}$$

Results are graphically illustrated in Figures 10 to 12 for Quarterly/Quarterly/Quarterly valve test frequency of the overspeed protection system. Figure 10 compares the external missile probability including overspeed with the NRC limit of 1E-5 per year for an unfavorably oriented unit as a function of the inspection interval in hours. Figure 11 compares the external missile probabilities for normal operation up to and including 120% speed with the NRC limit. Figure 12 compares the internal burst probability at normal operation up to and including 120% speed with inspection interval.

The above plots illustrate that as long as no cracking is detected, the unit can be safely operated for 100,000 hours between inspections.

FIGURE 10

13.9m^2 DESIGN

COMPARISON OF EXTERNAL MISSILE PROBABILITIES INCLUDING OVERSPEED WITH NRC LIMIT

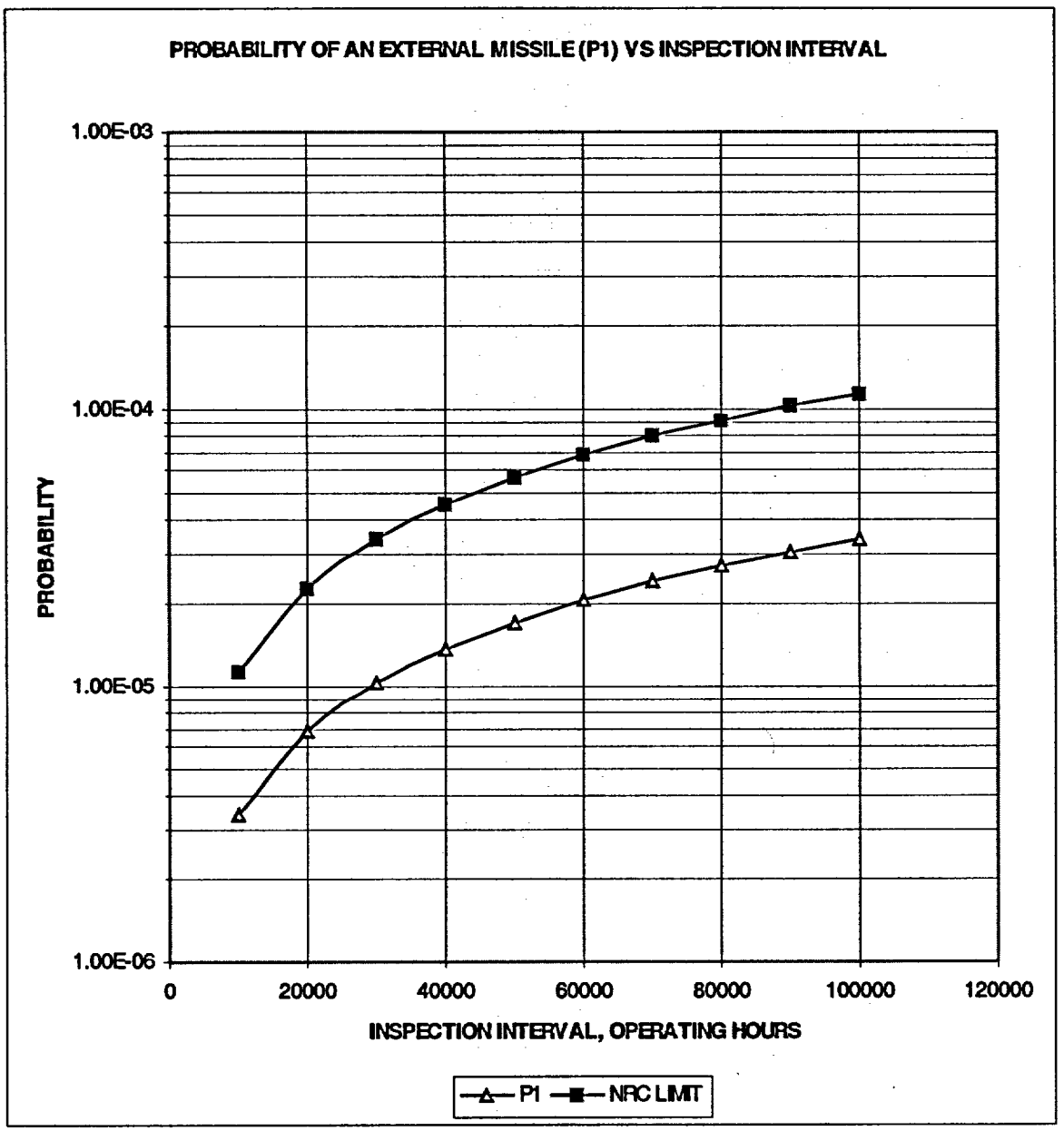

FIGURE 11

13.9 m^2 DESIGN

COMPARISON OF EXTERNAL MISSILE PROBABILITIES FOR NORMAL OPERATION UP TO 120% SPEED WITH NRC LIMIT

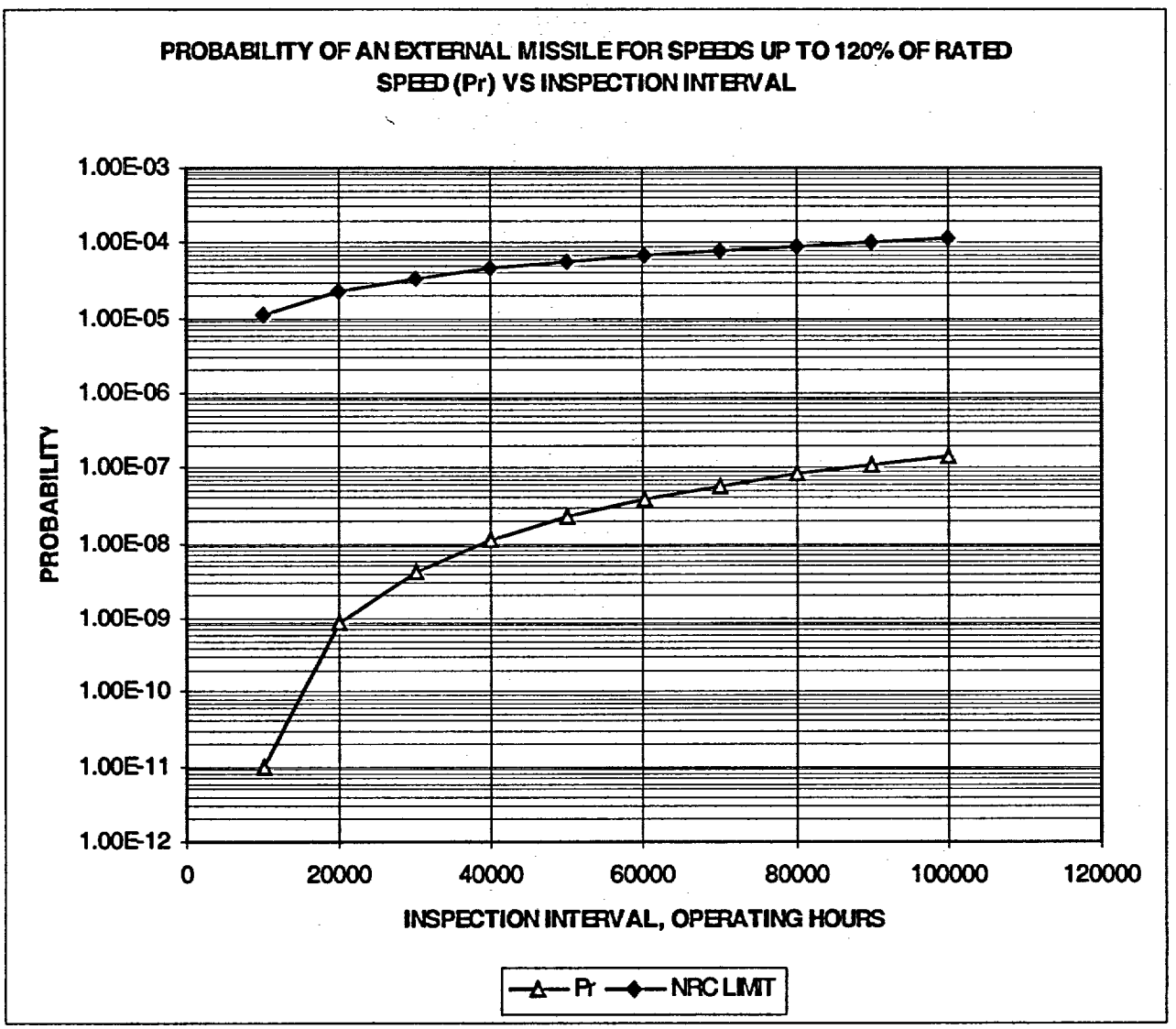

FIGURE 12

13.9 m^2 DESIGN

DISC BURST PROBABILITY AT NORMAL OPERATION UP TO 120% SPEED
VS INSPECTION INTERVAL

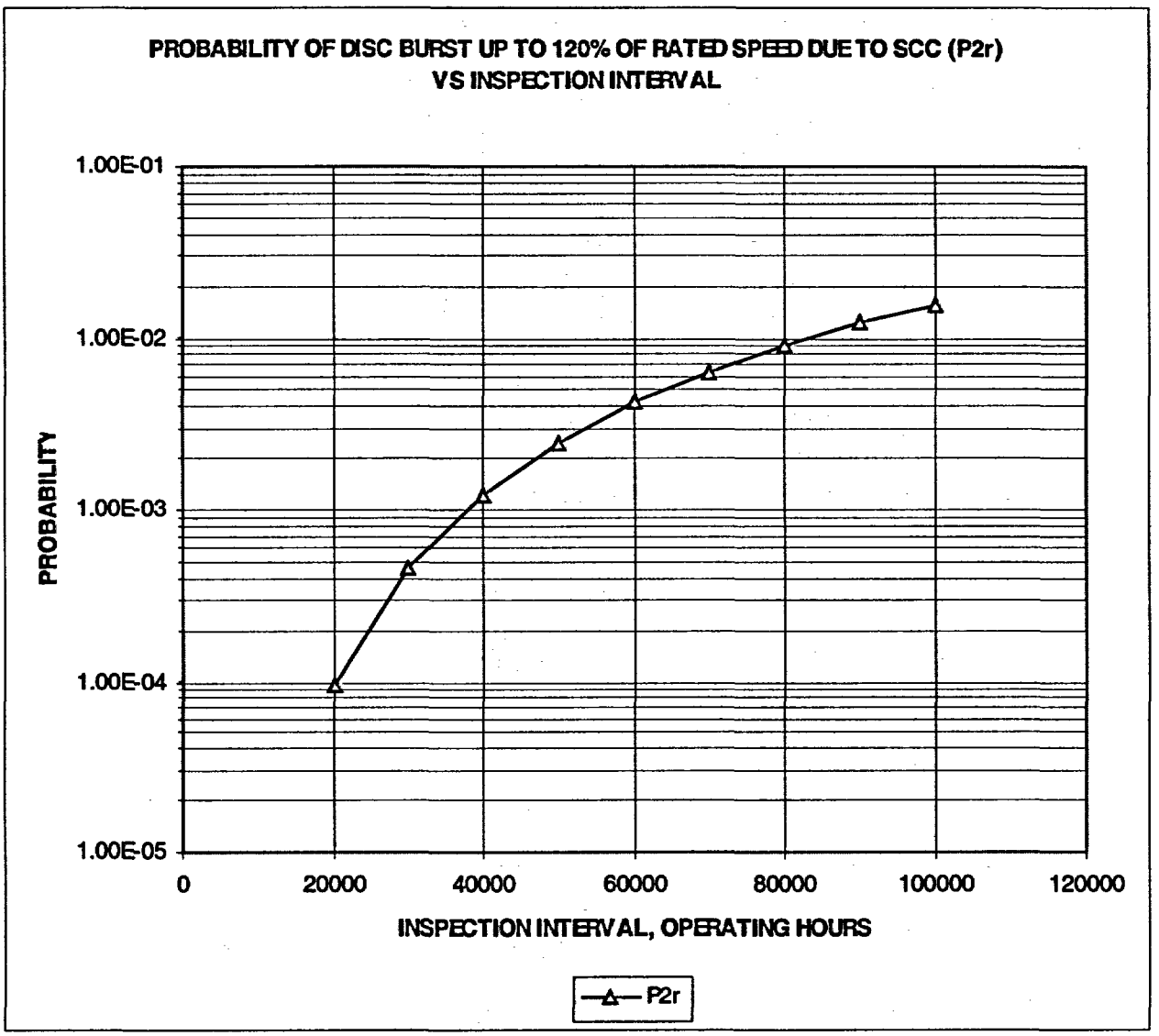

7 Conservatism in Methodology

Some conservatism's used in this report's assumptions and analysis are:

1. Residual compressive stresses introduced during manufacturing are conservatively assumed to be about –100 MPa. Figure 7 shows more realistic values of compressive residual stresses, which are much higher. The shrink fit and centrifugal stresses during normal operation, when combined with residual compressive stresses will reduce the final stresses to well below the threshold for stress corrosion cracking.
2. The crack initiation probabilities are based on the "old approach", which is applicable to ten and eight disc designs. Crack initiation probabilities could have been based on the "modern approach" with more up to date crack initiation data. This would have significantly lowered the probabilities.
3. Westinghouse crack growth rates are used in the analysis. These crack growth rates are the most conservative available.
4. The probability of achieving speeds up to 120% of rated speed during normal operating conditions is conservatively assumed to be 1.0. More realistically, the probability of achieving speeds from 100% up to 120% of rated speed is a small value typically less than about 2E-3. Speeds exceeding 107% to 110% by control system design are uncommon. Speeds above 100% are limited by generator synchronization.
5. The missile probability up to 120% speed and burst capability curves shown in Figures 11 and 12 are conservative at inspection intervals approaching 100,000 operating hours since they essentially represent the probability of a crack size exceeding 100 mm and not necessarily failure as discussed in section 3.4.
6. The probabilities of both burst and casing penetration for a run-away overspeed event greater than 120% of rated speed are conservatively set to be 1.0 for all discs. In reality, only the heaviest pieces with the worst geometry at significantly higher than 120% speed would penetrate the casing below the final burst speed. And then even less that 50% of those missiles would be thrown upward as downward trajectory missiles would impact balance of plant equipment only, such as the condenser.

8 References

[1] "Engineering Report ER-8402, "Probability of Disk Cracking Due to Stress Corrosion -- Comanche Peak Unit 1", Utility Power Corporation Proprietary Information, August 1984.

[2] "Engineering Report ER-8605a, "Probability of Disk Cracking Due to Stress Corrosion - Connecticut Yankee Replacement LP Rotors", Utility Power Corporation Proprietary Information, July 1986, Rev A, June 1987.

[3] "Engineering Report ER-8611, "Turbine Missile Analysis for 1800 rpm Nuclear LP-Turbines with 44-inch Last Stage Blades", Utility Power Corporation Proprietary Information, July 1986, Rev 1, June 1987.

[4] "Engineering Report ER-8503, "Probability of Disk Cracking Due to Stress Corrosion -- Grand Gulf Unit 1", Utility Power Corporation Proprietary Information, March 1985.

[5] "Energy Analysis in the Hypothetical Case of a Wheel Disk Burst in the LP Sections 1 to 3 of the New Design Series - Nuclear Power Plant Grand Gulf, 7153", Siemens Power Corporation Proprietary Information, June 1995.

[6] "Engineering Report ER-98044j, "Missile Analysis with LP Upgrade Grand Gulf Nuclear Unit No. 1", Proprietary Information of Siemens Fossil Power Corporation, November 1998.

[7] U.S. Nuclear Regulatory Commission, Regulatory Guide (RG) 1.115, U.S. Nuclear Regulatory Commission, NUREG-0800, "Standard Review Plan for the Review of Safety Analysis Reports for Nuclear Power Plants", July1981.

[8] U.S. Nuclear Regulatory Commission NUREG - 1048 including Appendix U & Table U.1.

[9] ABAQUS/Standard, HKS, 2001.

[10] W. G. Clark etc., ASME Paper "Procedures for Estimating the Probability of Steam Turbine Disc Rupture from Stress Corrosion Cracking", October 4-8, 1981.

[11] "Missile Probability Analysis Methodology for Limerick Generating Station, Unit 1&2 with Siemens Retrofit Turbines", June 18, 1997.

[12] "NN : Probability of Missile Generation in General Electric Nuclear Turbines – Supplementary Report: Steam Valve Surveillance Test Interval Extension – Non-proprietary Version GET-8039.1, September 1993.

[13] Ornstein, H. L.: "Operating Experience Feedback Report – Turbine-Generator Overspeed Protection Systems", U.S. Nuclear Regulatory Commission Report, NUREG-1275, Vol. 11, 1995.

[14] W. David, J. Ewald, F. Schmitz: „Grenzbelastungen zur Vermeidung von Spannungsrißkorrosion an ferritischen Rotorwerkstoffen", VGB-Konferenz „Korrosion und Korrosionsschutz in der Kraftwerkstechnik", 29. und 30. November 1995, Essen.

[15] W. David, J. Ewald, F. Schmitz: „Grenzbelastungen zur Vermeidung von Spannungsrißkorrosion an ferritischen Rotorwerkstoffen", Korrosionsschäden in Kraftwerken, 9. VDI Jahrestagung Schadensanalyse, 1. und 2. Oktober 1997, Würzburg.

[16] Letter from Mr. Bartholomew C. Buckley, NRC Senior Project Manager to Mr. George A Hunger, Jr., PECO Energy Company Director of Licensing, dated February 3, 1998, Subject: Limerick Generating Station (LGS), Units 1 and 2 of Main Turbine Rotor Replacement, Extension of Turbine Rotor Inspection Intervals and Valve Testing Frequencies (TAC Nos. M99341 and M99342).

[17] „Safety Evaluation of the Submittal to Replace Turbine Rotors at the Limerick Generating Station Units 1 and 2", NRC Docket Nos. 50-352 and 50-353.

[18] Letter from Mr. Herbert N. Berkow, NRC Director, to Mr. Stan Dembkoski, SWPC Director, dated July 22, 2003, Subject: Safety Evaluation for Acceptance of Referencing the Siemens Westinghouse Topical Report, "Missile Analysis Methodology for General Electric (GE) Nuclear Steam Turbine Rotors by the Siemens Westinghouse Power Corporation (SWPC)", TAC No. MB5679.

[19] Safety Evaluation by the Office of Nuclear Reactor Regulation, Siemens Westinghouse Topical Report "Missile Analysis Methodology for General Electric (GE) Nuclear Steam Turbine Rotors by the Siemens Westinghouse Power Corporation (SWPC)", Project 721.